

The Status of Supersymmetry after the LHC Run 1

Philip Bechtle[†], Tilman Plehn[‡] and Christian Sander[¶]

[†]Physikalisches Institut, Universität Bonn, Nussallee 12, 53115 Bonn, Germany

[‡]Institut für Theoretische Physik, Universität Heidelberg, Philosophenweg 16, 69120 Hamburg, Germany

[¶]Institut für Experimentalphysik, Universität Hamburg, Luruper Chaussee 149, 22761 Hamburg, Germany

Abstract. Supersymmetry (SUSY) is a complete and renormalisable candidate for an extension of the Standard Model. At an energy scale not too far above the electroweak scale it would solve the hierarchy problem of the SM Higgs boson, dynamically explain electroweak symmetry breaking, and provide a dark-matter candidate. Since it doubles the Standard Model degrees of freedom, SUSY predicts a large number of additional particles, whose properties and effects on precision measurements can be explicitly predicted in a given SUSY model. In this review the motivation for SUSY is outlined, the various searches strategies for SUSY particles at the LHC are described, and the status of SUSY in global analyses after the LHC Run 1 is summarized.

Contents

1	A Short Motivation	1
2	Theoretical Introduction	2
3	Generic Searches for Supersymmetry	6
4	SUSY Searches for Electroweak and Third-Generation Production	11
5	Exotic SUSY Scenarios	20
6	Current Status	22
7	Summary	27

1 A Short Motivation

In many ways, the Standard Model (SM) including a Higgs boson [2–6] is a complete theory, both from an experimental and from a theoretical point of view. It explains all observations at the LHC and at preceding high-energy experiments and shows no conceptual inconsistencies. Even better, it is a renormalisable field theory with all gauge couplings remaining perturbative to the Planck scale $M_{\text{Pl}} \sim 10^{19}$ GeV. Aside from gravity—which is missing in the Standard Model—we could be happy with this rather complete picture after the Higgs discovery [7]. However, if the perturbatively renormalisable Standard Model is supposed to describe all measurements in particle physics over such a wide range of energies, it looks much less complete [8, 9].

If we widen our experimental horizon beyond LHC energies, several shortcomings arise: Most notably, it does not explain dark matter [10, 11]; it does not accommodate the matter-antimatter asymmetry of the universe [12]; and it gives no reason why the three gauge couplings of the Standard Model gauge group almost meet at a large unification scale, but not quite [13].

Gauge coupling unification can be viewed as an experimental motivation for physics beyond the Standard Model, but it is closely tied to a list of open theoretical questions: Where does the flavour structure in the quark and lepton sectors come from? Is there a high-scale simplification of the Standard Model gauge structure? Why is the Higgs mass so much smaller than the Planck scale, which we consider the ultimate physical cut-off scale of the theory [14–16]?

Originally published in “The Large Hadron Collider — Harvest of Run 1”, edited by T. Schörner-Sadenius, Springer, 2015, pp. 421–462 [1].

As the only fundamental scalar particles in the Standard Model, the newly discovered Higgs boson causes peculiar problems in its perturbative field theory description. In the presence of a physical cut-off scale, its mass turns out to be extremely sensitive to quantum corrections. This means that we would expect such a scalar to acquire a mass close to the cut-off scale. On the other hand, electroweak symmetry breaking and the unitarity of WW scattering require the Higgs mass to stay sufficiently below the TeV scale. This tension is called the “gauge hierarchy problem” or “hierarchy problem”.

Supersymmetry is a leading candidate for a theory that can solve many of these problems [17–20]. It is based on an extension of the symmetry structure of the Standard Model by a symmetry linking fermions and bosons, i.e. matter fields and force carriers [21]. In that sense, supersymmetry completes the concept of symmetries as the guiding principle of elementary particle physics. While models with more than one supersymmetry generator are useful tools to study the structure of gauge theories, we will focus on the phenomenologically most interesting case of $\mathcal{N} = 1$ supersymmetry [22, 23].

This supersymmetric version of the Standard Model [8, 24, 25] protects the Higgs-boson mass from quadratic divergences. It improves the unification of the three gauge couplings and moves the gauge-unification scale to values around $M_{\text{GUT}} \simeq 10^{16}$ GeV, large enough to avoid predicting unobserved proton decays [26–29]. It can provide a weakly interacting dark-matter candidate, and it might help explaining the matter-antimatter asymmetry. And what makes it most relevant to LHC physics: It predicts new fundamental particles at the TeV scale.

2 Theoretical Introduction

The minimal supersymmetric Standard Model (MSSM) is the simplest supersymmetric extension of the Standard Model. Through the additional symmetry requirement it first of all doubles the number of fundamental particle fields. Since its underlying symmetry respects the number of degrees of freedom, it predicts two complex scalar fields for each Standard Model fermion, which can be arranged to match the two helicities of the Dirac field. For each Standard Model fermion f we denote these two scalar “sfermions” as $\tilde{f}_{L,R}$. The gauge bosons get mapped onto fermionic fields, where the massless photon and gluon fields only provide enough degrees of freedom for Majorana partners. This means that the discovery e.g. of a strongly interacting Majorana gluino \tilde{g} would be a clear sign for an underlying supersymmetry.

2.1 Minimal Supersymmetric Standard Model

Two additional aspects of the MSSM that are of crucial relevance to LHC searches are also directly linked to the properties of supersymmetric gauge theories.

First, the so-called superpotential, written in terms of superfields with their fermionic and bosonic constituent fields, predicts interactions where (scalar) supersymmetric partner states of quarks (squarks) and leptons (sleptons) are coupled to two Standard Model fermions. These interactions break lepton number and baryon number and mediate rapid proton decay. The easiest way to remove them is by postulating a new symmetry or multiplicative quantum number, called R -parity. All Standard Model states are assigned $R = +1$, which means they transform even under an R -transformation. In contrast, supersymmetric partner states with $R = -1$ are odd. R -parity thus requires that any interaction vertex include an even number of supersymmetric partner states [30, 31]. If, for example, we consider supersymmetric QCD with R -even quark and gluon fields and R -odd (scalar) quark partners \tilde{q} and (fermionic) gluon partners \tilde{g} , the allowed supersymmetric 3-point gauge interactions are

$$qqg, ggg \xrightarrow{\text{SUSY}} \tilde{q}\tilde{q}g, q\tilde{q}\tilde{g}, \tilde{g}\tilde{g}g.$$

Three-squark interactions do not exist because they would lead to proton decay and need to be forbidden. In addition, R -parity has a crucial effect on the “lightest supersymmetric partner” (LSP): As an R -odd state, it cannot decay to two Standard Model particles. Since, however, there is also no lighter supersymmetric partner to which it could decay through an allowed interaction, it has to be stable and can therefore serve as a dark-matter candidate.

Second, because of the underlying supersymmetry, the superpotential has to be holomorphic, i.e. it cannot include a superfield and its complex conjugate at the same time. This property directly translates into the Higgs scalar as a constituent of the superfield. The Higgs sector in the Standard Model gives mass to up-type and down-type fermions through the Higgs field and its conjugate. In the MSSM this is not possible, which means that the Standard Model ($R = +1$) sector of the MSSM has to be modified [32, 33]: Instead of one Higgs doublet we need at least two doublets to provide masses to all fermion fields. In the

State	Symbol	R	$SU(3)_c$	Q_{EM}
CP -even Higgs	h^0, H^0	+1	1	0
CP -odd Higgs	A^0	+1	0	0
charged Higgs	H^\pm	+1	1	± 1
gluino	\tilde{g}	-1	8	0
neutralinos	$\tilde{\chi}_1^0, \tilde{\chi}_2^0, \tilde{\chi}_3^0, \tilde{\chi}_4^0$	-1	1	0
charginos	$\tilde{\chi}_1^\pm, \tilde{\chi}_2^\pm$	-1	1	± 1
up squarks	$\tilde{u}_{L,R}, \tilde{c}_{L,R}, \tilde{t}_{1,2}$	-1	3	$2/3$
down squarks	$\tilde{d}_{L,R}, \tilde{s}_{L,R}, \tilde{b}_{1,2}$	-1	3	$-1/3$
sleptons	$\tilde{e}_{L,R}, \tilde{\mu}_{L,R}, \tilde{\tau}_{1,2}$	-1	1	± 1
sneutrinos	$\tilde{\nu}_e, \tilde{\nu}_\mu, \tilde{\nu}_\tau$	-1	1	0
gravitino	\tilde{G}	-1	1	0

Table 1. MSSM mass eigenstates after electroweak symmetry breaking. We assume that left-right scalar mixing is only relevant for the massive third generation.

minimal setup of the MSSM, these doublets are arranged such that at tree level one of them couples to up-type fermions and the other to down-type fermions. In combination, their two vacuum expectation values have to provide the weak gauge boson masses, $v_u^2 + v_d^2 = v^2 = (246 \text{ GeV})^2$. Two complex Higgs doublets are built of eight degrees of freedom. Just as in the Standard Model, one pseudo-scalar degree of freedom and one set of charged degrees of freedom become the Goldstone modes of the massive Z and W^\pm bosons. The remaining five degrees of freedom, including a pseudoscalar and a charged scalar, turn into physical Higgs fields: two scalar Higgs fields H_1^0 and H_2^0 , one pseudo-scalar Higgs A^0 , and a pair of charged Higgs fields H^\pm . The two scalar states mix to mass eigenstates, h^0 and H^0 . As will be discussed below, the mass of the lightest supersymmetric Higgs boson is bounded from above.

In particular the structure of scalar interactions in the MSSM is not obvious from the Standard Model Lagrangian. The reason is that supersymmetry respects the number of degrees of freedom not only of the on-shell particles, but also of the off-shell fields. Already in the simple Wess–Zumino model [19] with its chiral (matter) superfield, we observe that the conservation of off-shell degrees of freedom as well as the consistency of supersymmetry transformations staying within each superfield require an auxiliary field F . It does not feature a kinetic term and can therefore be removed through its equation of motion. After integrating out the F field, this structure ensures that the Standard Model matter fermions and their scalar partners have the same masses. If we include gauge interactions via a vector superfield this links the Standard Model gauge bosons to their fermionic gaugino partners and leads to another auxiliary field, D . This field has gauge couplings to scalars of the kind $D\phi^\dagger\phi$, which after exploiting the equation of motion introduces gauge couplings of the type ϕ^4 . In the Higgs sector they replace the free quartic coupling $\lambda\phi^4$ and hence determine the masses of the supersymmetric Higgs bosons. After diagonalising the Higgs eigenstates, we can express the mass of the lightest Higgs boson in terms of the ratio of the two vacuum expectation values $\tan\beta = v_u/v_d$, namely [34–37]

$$M_h = M_Z \cos(2\beta) + \text{radiative corrections} < 135 \text{ GeV}, \quad (1)$$

where the limit assumes squarks in the TeV range. This is one of the key predictions of the MSSM and is based on the structure of its scalar potential. In the light of the experimental constraints discussed in section 6.1, the additional MSSM Higgs states should be significantly heavier.

If we add supersymmetric partners for the entire Standard Model spectrum, keeping in mind that the two Higgs doublets are R -even, we find the MSSM particle content shown in table 1. As mentioned before, every Standard Model fermion acquires a scalar partner, called squark, slepton or sneutrino. The first-generation and second-generation sfermions with their negligible fermion-Higgs couplings can, to a good approximation, be represented by their interaction states, while the heavy-flavour sfermions have to be rotated into their mass eigenstates. This follows from the structure of their masses and mixings, which is determined by supersymmetry breaking.

Every Standard Model boson matches onto a fermionic partner; one example is the gluino as the partner of the gluons. Because supersymmetry respects the number of degrees of freedom, an on-shell gluino without counting the colour structure can only be made out of two degrees of freedom. This does not allow us to define a Dirac fermion and leaves us with a Majorana fermion, which forms its own anti-particle. In the interaction basis the partner states of the electroweak gauge bosons and the extended Higgs sector occur as one neutral bino, charged and neutral winos, and charged and neutral Higgsinos. These states can mix into mass eigenstates, called neutralinos and charginos and ordered by mass. The neutralinos, just like the gluino, are Majorana fermions, as suggested by the available two on-shell degrees

of freedom. The charginos with their electric charge cannot be their own anti-particles, so they instead form Dirac fermions with interactions that violate particle number. Finally, the gravitino as the spin-3/2 partner of the graviton can play a role at the LHC in specific supersymmetric models.

2.2 Supersymmetry Breaking

Obviously, supersymmetry is not an exact symmetry of nature, because we have not observed any scalar partners of the Standard Model fermions with the same masses. Without affecting the stabilisation of the quadratically divergent Higgs mass and the improved gauge coupling unification, we can introduce masses for all supersymmetric partners through so-called soft breaking [38]. In this way, the supersymmetric partners receive two contributions to their masses from electroweak symmetry breaking as well as from soft supersymmetry breaking. Such soft-breaking masses remove the quadratic divergence of the Higgs mass, but leave a logarithmic dependence. The largest contribution to the light Higgs mass is proportional to the logarithm of the top-stop mass ratio, $\log(m_{\tilde{t}}/m_t)$. This logarithmic mass dependence leads to the dominant radiative corrections in equation (1) and is referred to as the “little hierarchy problem” of supersymmetry. It is a key ingredient to so-called naturalness arguments. In general, naturalness describes to what degree we have to tune ratios of model parameters in order to accommodate experimental constraints on a model. If the light Higgs mass given in equation (1) is considered a prediction over the MSSM parameter space, a large stop mass moves us away from the supersymmetric limit $m_t = m_{\tilde{t}}$ and is hence fine-tuned or un-natural. While a discussion of these effects will be part of a theoretical analysis of a given supersymmetric model after its discovery, its benefit in guiding LHC analyses is not at all obvious.

Including the soft breaking terms, the relevant Lagrangian of the MSSM reads [8]

$$\begin{aligned}
-\mathcal{L}_{\text{soft}} = & m_{H_d}^2 |H_d|^2 + m_{H_u}^2 |H_u|^2 - (B\mu H_u \cdot H_d + \text{h.c.}) \\
& + m_{\tilde{Q}}^2 |\tilde{Q}|^2 + m_{\tilde{U}^c}^2 |\tilde{U}^c|^2 + m_{\tilde{D}^c}^2 |\tilde{D}^c|^2 + m_{\tilde{L}}^2 |\tilde{L}|^2 + m_{\tilde{E}^c}^2 |\tilde{E}^c|^2 \\
& + \left(y_u A_u \tilde{Q} \cdot H_u \tilde{U}^c - y_d A_d \tilde{Q} \cdot H_d \tilde{U}^c - y_e A_e \tilde{L} \cdot H_d \tilde{E}^c + \text{h.c.} \right) \\
& + \left(\frac{M_3}{2} \tilde{g}^a \tilde{g}^a + \frac{M_2}{2} \tilde{W}^d \tilde{W}^d + \frac{M_1}{2} \tilde{B}^0 \tilde{B}^0 + \text{h.c.} \right), \tag{2}
\end{aligned}$$

where we omit flavour indices. The first line contributes to the Higgs potential, as do the supersymmetric F and D terms described above. The second and third lines generate masses and mixings for the sfermions. The couplings of the kind $y_j A_j$ describe left-right mixing in the Higgs interaction and turn into mixing terms in the squark-mass matrix after electroweak symmetry breaking. Assuming that they are proportional to the fermion Yukawa interaction ensures that the one-loop contributions to the fermion masses are protected by the chiral symmetry, i.e. they scale with the fermion masses themselves. In table 1 we neglect them for the first two generations. The final line in the Lagrangian (2) contains three gaugino Majorana mass terms.

If we expand the Lagrangian (2) in its most general form, the number of free parameters exceeds 100, which makes the MSSM scenario somewhat un-predictive. This parameter set includes complex gaugino masses and trilinear mixing parameters, which are strongly constrained by electric dipole moments, or a general flavour sector with 6×6 matrices for the squark masses, clearly not reflecting the observed flavour symmetries. For direct LHC searches with their given energy range and their limited precision, we can reduce this set to the LHC-relevant parameters, usually referred to as the phenomenological MSSM (pMSSM). Its specific assumptions are: no R -parity violation, no new sources of CP violation, mass-degenerate first and second generation scalars, and no flavour-changing neutral currents. These assumed symmetry properties automatically avoid a large number of indirect constraints on the supersymmetric Lagrangian and allow for a dark-matter candidate. They leave us with 19 supersymmetric model parameters at the TeV scale:

Higgs potential parameters: $\tan \beta$, μ , and M_A ;
gaugino masses: M_1 , M_2 , and M_3 ;
squark mass parameters: $m_{\tilde{t}_L}, m_{\tilde{t}_R}, m_{\tilde{b}_R}, m_{\tilde{u}_L}, m_{\tilde{u}_R}$, and $m_{\tilde{d}_R}$;
slepton and sneutrino mass parameters: $m_{\tilde{\tau}_L}, m_{\tilde{\tau}_R}, m_{\tilde{e}_L}$, and $m_{\tilde{e}_R}$;
trilinear couplings: A_t, A_b , and A_τ .

In the pMSSM, the lightest neutralino is the dark-matter candidate [39, 40], because the only other weakly interacting candidate, sneutrino dark matter, is ruled out experimentally. The gravitino only

couples gravitationally to the rest of the spectrum. As long as it is not the LSP, it will therefore not play a role in LHC phenomenology. However, if it should be the LSP and lead to decays of long-lived particles, it can easily be added to the pMSSM.

At the TeV scale, all pMSSM parameter can be chosen independently. However, if we attempt to link these model parameters to the structure of supersymmetry breaking, we will most likely evolve them to higher energy scales, above which supersymmetry will remain unbroken. Under renormalisation group evolution the squark and gluino masses behave differently: The gluino mass only receives multiplicative corrections, while the squark mass gets corrected by terms proportional to the gluino mass. In this way a heavy gluino will induce large squark masses, which means that we cannot link models with $m_{\tilde{g}} \gg m_{\tilde{q}}$ to high-scale theories [41]. To a lesser extent the same is true for sleptons and electroweak gauginos. From a phenomenological perspective this does not cause any problems, because indirect constraints mostly require heavy scalars. The extreme case of decoupled sfermions is referred to as “split supersymmetry” [42, 43], and will be discussed in section 5.1.

Historically, many searches for supersymmetry were not only interpreted, but also set up with a specific SUSY-breaking mechanism in mind. Actual supersymmetry breaking can be described by the auxiliary F and D fields introduced in section 2.1. However, for LHC phenomenology supersymmetry breaking is simply an experimental fact; what is more relevant is the way supersymmetry breaking is mediated to the TeV-scale Lagrangian. The most popular mechanism is gravity mediation, either referred to as a supergravity-inspired model (mSUGRA) or as a strongly constrained minimal supersymmetric model (CMSSM). In these models the sector communicating SUSY breaking does not couple to the gauge structure of the Standard Model [44–46]. This requires all gaugino masses, all scalar mass parameters (of Higgs bosons, squarks and sleptons) and all trilinear couplings to unify at the same scale. The CMSSM model parameters are $m_{1/2}$, m_0 , and A_0 , all defined at M_{GUT} . In addition, we specify $\tan\beta$ and the sign of μ in the Higgs sector. Strictly speaking, in the corresponding mSUGRA model the free model parameter is $B = A_0 - m_0$. After renormalisation group evolution, the gaugino masses in the CMSSM scale with constant ratios M_i^2/g_i^2 , or $M_1 : M_2 : M_3 \sim 1 : 2 : 6$. The lightest squark will be the lighter stop, its TeV-scale mass mostly depending on $m_{1/2}$. The gravitino is similar in mass to the other superpartners and usually does not affect the LHC phenomenology significantly because it is not the LSP. A variant of the CMSSM is the non-universal Higgs mass ansatz (NUHM), which separates the scalar supersymmetric partner masses from the scalar Higgs sector.

An alternative breaking mechanism is gauge mediation (GMSB). If we assume that some kind of messenger sector communicates SUSY breaking to the MSSM spectrum, gravity mediation assumes that this messenger sector is not charged under any of the Standard Model charges. In gauge mediation we allow for non-gravitational interactions between the SUSY breaking sector and the MSSM particles [47, 48]. The corresponding messenger particles can have masses in the 10^4 GeV range. Again, the gaugino masses scale like constant ratios M_i/g_i^2 . Gaugino masses and scalar squared masses are generated at the one-loop and two-loop levels such that eventually they are of similar size. The gravitino can be the LSP, which for the LHC means that the second-lightest supersymmetric partner (NLSP) can be long-lived before it eventually decays e.g. to a gravitino and a photon or an electroweak gauge boson.

In such a scenario where the NLSP is linked to the rest of the supersymmetric spectrum and the LSP is very weakly coupled, the lightest supersymmetric partner relevant for LHC analyses is different from the actual LSP at cosmological time scales. Now, the NLSP does not have to be electrically neutral, so the non-gravitational decay chains at the LHC can as well end with the lightest slepton. The question if we can observe and measure such late decays at the LHC depends on the lifetime of the NLSP.

2.3 Signatures of SUSY

While our theoretical understanding of supersymmetry breaking might make it appealing to search for CMSSM and GMSB signatures right away, we should instead identify the most generic features of supersymmetric models and search for those. In the spirit of the pMSSM, we can start with the straight-forward assumption that the LSP is the lightest neutralino and that it is responsible for (part of) the dark matter in the universe.

In that case we expect to see strongly and weakly interacting supersymmetric states at the LHC. Unless they are too heavy, the strongly interacting particles with production cross sections proportional to α_s^2 will be produced much more frequently than the weak states with cross sections proportional to $\alpha_W^2 \sim \alpha_s^2/250$. Some production cross sections are shown in figure 1 as a function of the mass of the produced supersymmetric particles. Because of the Majorana nature of the t -channel gluino exchange, squarks \tilde{q} and anti-squarks \tilde{q}^* can be produced in pairs as $pp \rightarrow \tilde{q}\tilde{q}^*$ and $pp \rightarrow \tilde{q}\tilde{q}$. Slepton-pair production is further suppressed because it can only proceed through s -channel diagrams. On the other hand, the

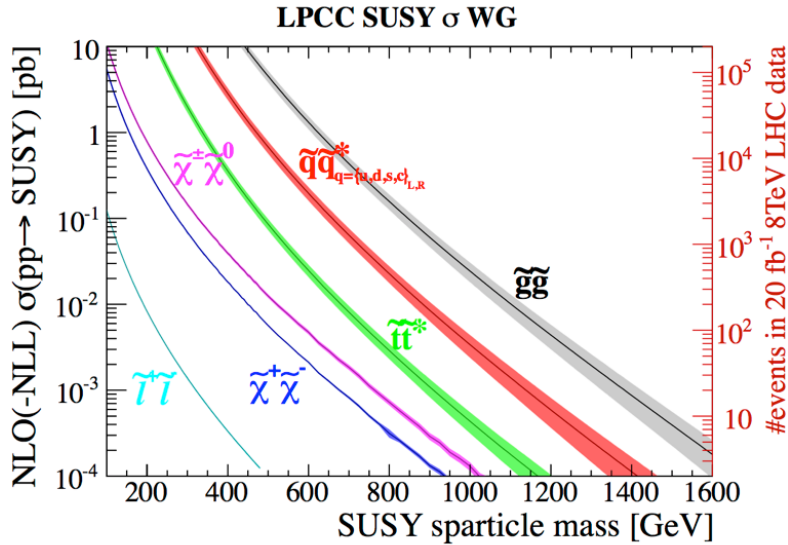


Fig. 1. The cross sections expected for different production modes of SUSY particles as a function of their mass. At the same mass scale, gluino production dominates over the production of first-generation squarks. Third-generation squark production is suppressed, since these particles cannot be produced in t -channel processes. Particles not participating in the strong interaction, like gauginos and sleptons, have the smallest production cross section. (*Adapted from Ref. [49].*)

LSP cannot be strongly interacting, which means that the directly produced coloured states first need to shed their colour charge by radiating jets, thus decaying to the weakly interacting sector, and then in turn decay to two LSPs. The resulting LHC signature consists of jets plus missing energy. A distinct advantage of this signature is that irreducible background cross sections like W +jets and Z +jets are not huge and produce much softer jets compared to the signal. Top-quark pairs can be a dangerous background and will then have to be suppressed, as described below.

Following the above argument of strongly interacting superpartner production with a cascade decay to the weak sector and the LSP at the end, such a decay chain starting from each gluino or squark could read

$$(\tilde{g} \rightarrow) \tilde{q} \rightarrow \tilde{\chi}_2^0 \rightarrow \tilde{\ell} \rightarrow \tilde{\chi}_1^0. \quad (3)$$

The corresponding classic kinematic signature for cascade decays arises from the two leptons: two same-flavour opposite-sign leptons with an invariant mass below an edge given by

$$0 < m_{\ell\ell}^2 < \frac{(m_{\tilde{\chi}_2^0}^2 - m_{\tilde{\ell}}^2)(m_{\tilde{\ell}}^2 - m_{\tilde{\chi}_1^0}^2)}{m_{\tilde{\ell}}^2}. \quad (4)$$

Typical backgrounds are $\gamma^*/Z^0 \rightarrow \ell^+\ell^-$ events as well as leptonically decaying top-quark pairs. The latter can feature both same-flavour and opposite-flavour leptons, which means that they can be controlled by looking at the difference of the same-flavour and opposite-flavour events. The dominant Drell-Yan background for same-flavour leptons should be well understood experimentally and theoretically.

Changing the production process from light-flavour squarks or sbottoms to stop pairs leads to a very different decay signature, for example $\tilde{t} \rightarrow t\tilde{\chi}_1^0$ or $\tilde{t} \rightarrow b\tilde{\chi}_1^+$. The kinematic edge typical for cascade decays does not feature in this process, and the final state can be indistinguishable from top-quark pair production. Hence, in particular for small stop masses this signal is challenging to extract from the much larger top-pair background. Other ways of searching for supersymmetry, based on electroweak production processes, long-lived particles or R -parity violating decays will be discussed below.

3 Generic Searches for Supersymmetry

Given the large number of free parameters (see section 2.2), the MSSM in particular and SUSY in general have a plethora of realisations. As discussed before, there are various possible signatures and some of these provide a generic sensitivity to many SUSY models. In this section we discuss various classes of

such signatures and describe a few analysis methods used to estimate the remaining background from Standard Model processes after typical event selections.

3.1 Searches with Jets and E_T^{miss}

In proton-proton collisions, coloured sparticles are dominantly produced via the strong interaction—at least if they are not too heavy.

Although leptons can also be produced (see next section 3.2), fully hadronic decay chains have a large probability to be realised. The LSP at the end of the sparticle decay chain is only weakly interacting and therefore escapes the detector unseen, leaving a momentum imbalance in the transverse plane of the event. This imbalance manifests itself as the missing transverse energy E_T^{miss} of an event. Thus, searches in final states with jets and E_T^{miss} but without leptons are expected to have a good sensitivity to a large fraction of supersymmetric models.

In many cases, SUSY events are expected to produce on average more E_T^{miss} , or higher multiplicities of energetic jets. Consequently, searches for new physics are typically selecting events in the tails of distributions of E_T^{miss} and/or other observables, and these quantities have to be precisely understood. However, detector effects, misreconstruction or unknown higher-order corrections to the production of many additional partons in the final state are contributing to potentially large systematic uncertainties. To minimise this uncertainty, most of the searches are using data as much as possible to estimate the SM backgrounds from events in phase-space regions which are dominated by SM processes. An example for this approach is Ref. [50] which describes the search for new physics in final states with many jets and missing transverse energy. The background to this search has four major contributions:

Firstly, the irreducible background from $Z(\rightarrow \nu\nu)$ +jets events. This background can be estimated from selected $Z(\rightarrow l^+l^-)$ +jets events, by removing the two leptons from the event (as if they would be neutrinos) and correcting for lepton efficiencies and acceptance effects as well as for the ratio of the branching fractions of Z into neutrinos and Z into charged leptons. As this ratio is approximately six, this correction leads to large statistical uncertainty. Alternatively, γ +jets events can be used by exploiting their similarity to Z +jets events at high boson momenta where mass effects can be neglected. The statistical uncertainty for this method is significantly smaller, but the systematic uncertainties from unknown higher-order electroweak and QCD corrections on the cross section ratio of Z +jets and γ +jets are particularly large for high jet multiplicities.

Secondly, there is a background originating from W +jets and $t\bar{t}$ events with leptonically decaying W bosons, i. e. $W \rightarrow \ell\nu$ with $\ell = e, \mu$. The neutrino leads to genuine E_T^{miss} , and if the lepton is lost (i.e. not reconstructed, not isolated, or out of acceptance), the event can be selected. The background can be estimated from a μ +jets control sample by reweighting the events according to the muon inefficiencies, which are measured from data.

Thirdly, if a W in W +jets or $t\bar{t}$ events decays into a τ lepton and a neutrino, the τ can decay hadronically and leave a jet-like signature. This contribution can also be estimated from a μ +jets control sample by replacing the muon by a jet with a momentum expected from a hadronic tau decay. Corrections have to be applied for the muon reconstruction and isolation efficiencies, as well as for the branching ratio of the τ lepton into hadronic final states.

A final significant background is QCD multi-jet production with E_T^{miss} originating from jet energy mismeasurements. This background is estimated from an inclusive jet sample. Each event is, in a first step, rebalanced in the transverse plane, i.e. the jet momenta are adjusted within their uncertainties such that the event has no E_T^{miss} . In a second step, each jet is smeared according to measured jet energy response distributions. It is particularly important to include the non-Gaussian tails in the jet energy response, as they can lead to particularly large values of E_T^{miss} .

Finally, 36 exclusive search regions are defined in $H_T = \sum_{\text{jets}} p_T$, $H_T^{\text{miss}} = |\sum_{\text{jets}} \mathbf{p}_T|$, and N_{jets} .

Alternative methods for the background estimation are, for example, the usage of simulated events, which are then reweighted according to the ratio to data in background-dominated control regions.

A comparison of background prediction and data shows a good agreement (see figure 2), and since no signal is observed upper limits on sparticle masses are set in various supersymmetric models. If the results are interpreted in the CMSSM, as shown in figure 3(a), the fully hadronic searches are sensitive to squark masses up to 1.3 TeV and gluino masses up to 1.8 TeV. Mass limits in less constrained models can be significantly weaker, as will be discussed in section 3.4.

Many other analyses with different observables and analysis techniques have been carried out in the fully hadronic final state. One often used observable is $m_{\text{eff}} = H_T + E_T^{\text{miss}}$, which is an estimator for the total energy scale of the event [51]. Other variables are motivated by the process $\tilde{q}\tilde{q} \rightarrow q\tilde{\chi}_1^0 q\tilde{\chi}_1^0$ for which the two jets originating from the emitted quarks are possibly enclosing a small azimuthal angle

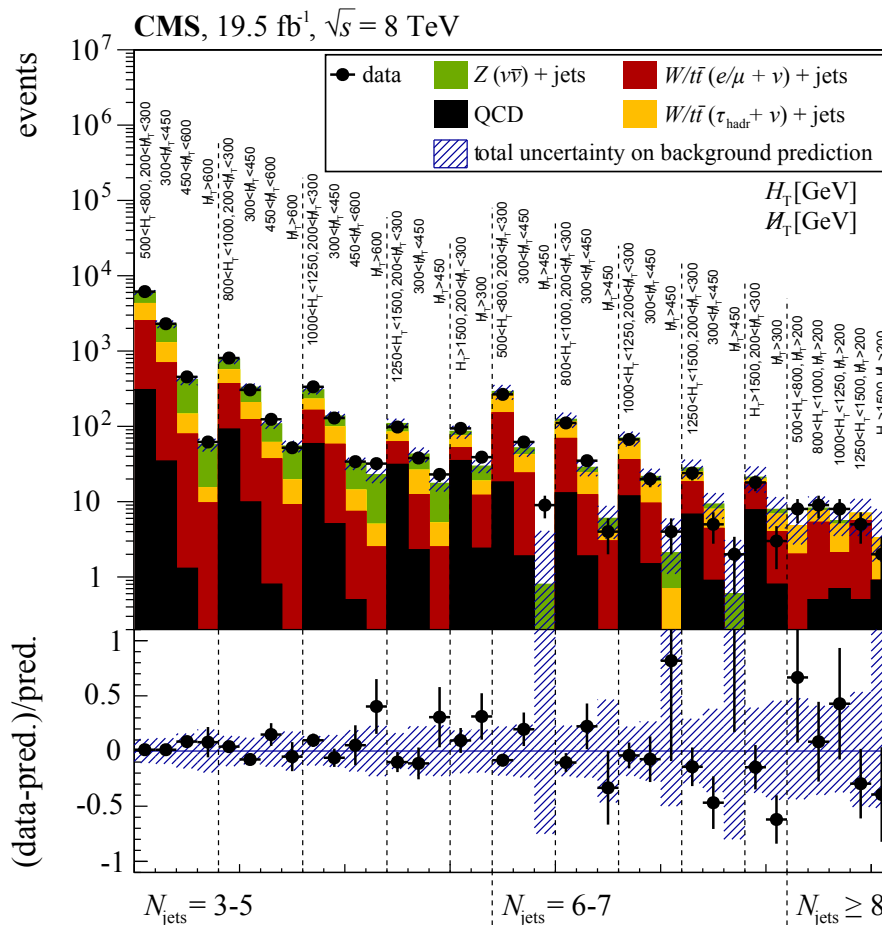


Fig. 2. Comparison of background prediction and data for various search regions defined in H_T , H_T^{miss} , and N_{jets} . (Adapted from Ref. [50].)

($< \pi$), while for QCD dijet events the two leading jets are mostly back-to-back in the transverse plane. Moreover, the momenta of the jets are carrying some information on the mass difference between the initially produced SUSY particles and the final-state LSPs. Therefore, the jet kinematics can be used to construct observables which are having a high potential to separate background from signal, and which are further sensitive to the scale of a given scenario of new physics. In the case of longer decay chains, the jets are clustered in two “hemispheres”, and for each of them the four momenta of the jets are added to one “pseudo-jet”. The resulting two pseudo-jets are then used for further kinematic investigations. Three of the variables which have been used in the fully hadronic channel are α_T [53, 54], the razor [55], and the “stransverse mass” m_{T2} [56–59], which is further explained in section 4. All the different approaches show a comparable sensitivity to new physics.

3.2 Final States with Leptons and E_T^{miss}

Leptons can be produced in supersymmetric decay chains either if sleptons are present in the sparticle decay chain or if heavier neutralinos or charginos occur. In the latter case, W and Z bosons can be produced, which can decay further into leptons. If the initially produced supersymmetric particle is a squark or a gluon, at least one jet per decay chain is produced, and thus another typical final-state signature for many supersymmetric models consists of jets+isolated leptons+ E_T^{miss} , where the isolation observable is calculated from further energy deposits in a cone around the lepton. We distinguish here between leptons of the first two generations (electrons and muons) and of the third generation (τ leptons) since the reconstruction of hadronically decaying τ leptons is more complex. Different lepton multiplicities and charge combinations are sensitive to different models: Single-lepton searches are quite generic, but

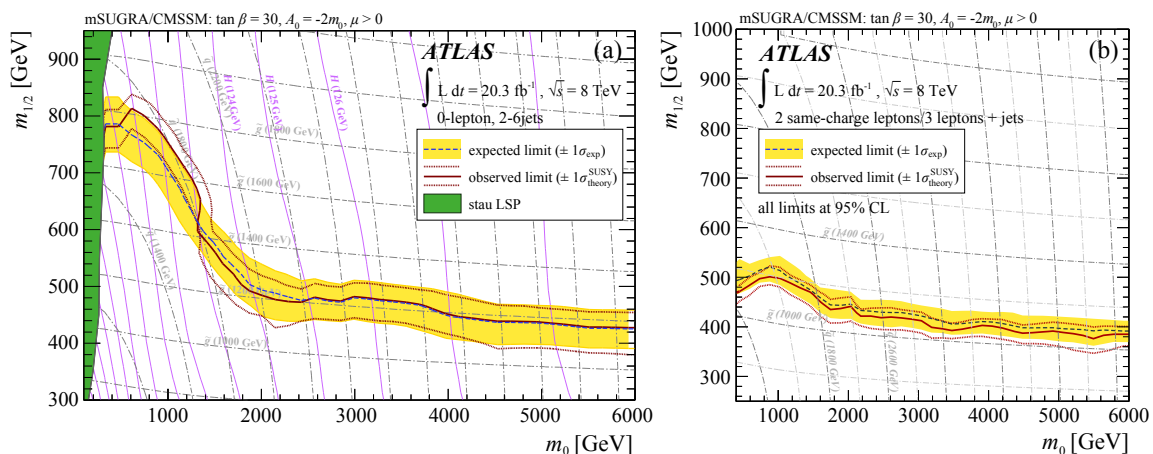


Fig. 3. Interpretation of ATLAS searches in final states with jets+ E_T^{miss} or jets+same-sign leptons+ E_T^{miss} in the CMSSM. (Adapted from Refs. [51, 52].)

often suffer from large backgrounds from Standard Model processes [60, 61]. Final states with three or more leptons are particularly sensitive to the direct production of electroweak superpartners, as will be discussed later. Final states with two leptons can be separated into different classes according to the lepton charges and flavours: same sign or opposite sign with same flavour or opposite flavour. In particular the searches in final states with same-sign leptons provide good sensitivity to many models, because in signal events the two leptons with the same charge can be produced in different decay chains, e. g. $\tilde{q}\tilde{q} \rightarrow \tilde{q}\tilde{q}\tilde{\chi}_1^\pm\tilde{\chi}_1^\pm \rightarrow \tilde{q}\tilde{q}l^\pm\nu l^\pm\nu\tilde{\chi}_1^0\tilde{\chi}_1^0$, while Standard Model same-sign processes are very rare and mostly originate from events where a non-prompt lepton, e. g. from a heavy-flavour jet, accidentally fulfills the isolation requirement [52, 62]. This background is usually estimated by selecting leptons with a looser isolation criterion and reweighting the events with a tight-to-loose ratio that has been measured in a background-enriched control region.

So far, no excess beyond the Standard Model expectation has been established at the LHC for searches in final states with leptons, jets and E_T^{miss} , and the results are interpreted in various models of supersymmetry. Figure 3(b) shows the interpretation in the CMSSM. While the jets+ E_T^{miss} searches provide the best sensitivity at small values of m_0 (see Figure 3(a)), the sensitivity of searches with same-sign leptons are almost independent of m_0 , and both searches exclude at large values of m_0 comparable regions in the m_0 - $m_{1/2}$ plane.

In many supersymmetric models the partner of the τ lepton, the stau ($\tilde{\tau}$) is the lightest slepton. Light staus that are almost mass-degenerate with the LSP are very interesting from a cosmological point of view as will be further explained in section 6.1. Thus, if staus are light, it is expected that they occur frequently in decay chains, and that consequently numerous τ leptons are produced. Signatures in which the τ lepton decays further into a light lepton and two neutrinos are covered by the searches with electrons and/or muons as described above. However, in $\sim 65\%$ of the cases, the τ decays into an odd number of charged hadrons accompanied by neutral hadrons. If the mass splitting between the stau and the LSP is small, the τ leptons can have rather low transverse momenta, and not all might be reconstructed. Therefore, searches with only one or with more τ leptons in final states with additional jets from the decay of the initially produced squarks or gluons and E_T^{miss} are motivated [63–65]. The dominant background for the search with one τ lepton are W +jets events and, to a smaller extent, QCD multi-jet events with one jet being misreconstructed as a hadronically decaying τ . For the final state with two τ leptons, the dominant backgrounds are again W +jets events with one real τ and one misidentified jet, as well as $t\bar{t}$ events with two real τ leptons. No evidence for new physics has been observed by ATLAS and CMS so far, and limits on supersymmetric parameters have been set. Two interpretations within the CMSSM and within the GMSB model are displayed in figure 4. Especially for the CMSSM interpretation it can be seen that the best sensitivity is observed for models where m_0 and thus the mass of the stau is small and close to the mass of the LSP.

Furthermore, a very generic search for anomalous production of three or four leptons in various flavour combinations and kinematic search regions, e.g. with low or high accompanying jet activity, has been performed [66]. Once more, no significant excess beyond the expected statistical fluctuations has been observed.

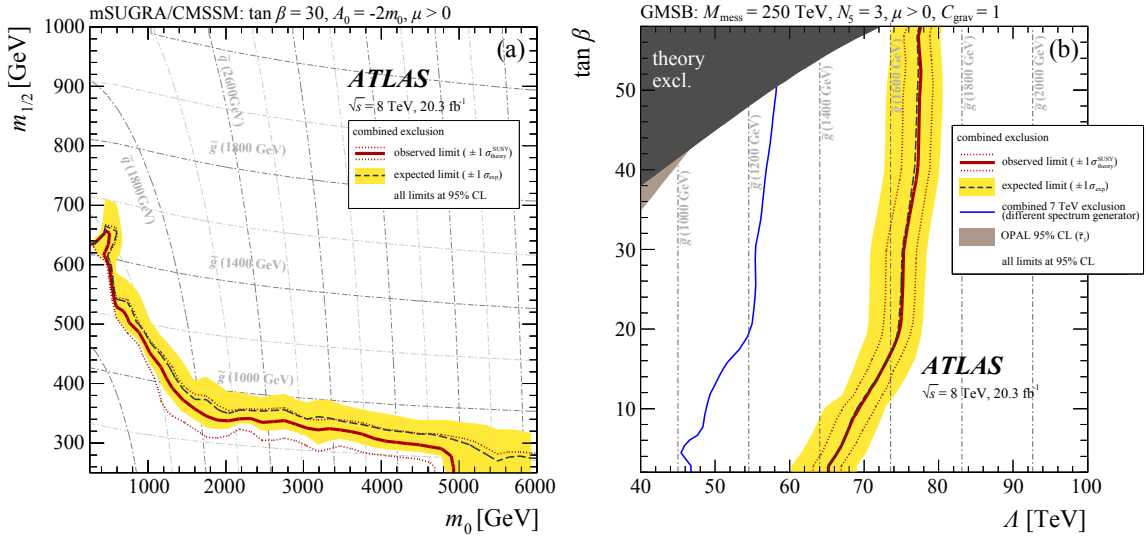


Fig. 4. (a) CMSSM interpretation of the ATLAS search with at least one τ lepton, E_T^{miss} and jets. The search performs best for small m_0 , i. e. small $\tilde{\tau}$ masses. (b) Interpretation of the same analysis in the GMSB; the limits are shown in the plane defined by the parameter $\tan \beta$ and the effective SUSY breaking scale Λ . (*Adapted from Ref. [65].*)

3.3 Final States with E_T^{miss} and Photons

In the searches discussed above, it was assumed that the LSP is the lightest neutralino. However, in GMSB models the gravitino is the LSP [67]. As—due to the weakness of gravitation—the couplings of the gravitino to other particles are heavily suppressed, all decay chains are reaching the next-to-lightest supersymmetric particle (NLSP), which then decays further into the gravitino and a SM particle. The type of this SM particle is related to the type of the NLSP: If the NLSP is “bino-like”, the SM particle will most likely be a photon, while for “wino-like” NLSPs it will in most cases be a Z boson. This fact motivates searches for supersymmetry in final states with one or more photons in association with jets and E_T^{miss} . Important backgrounds for such searches are originating from photon+jet processes with jet energy mismeasurement leading to artificial E_T^{miss} , from QCD multi-jet production where one of the jets is identified as a photon, and lastly from $W(\rightarrow e\nu)$ +jets production with the electron being misreconstructed as a photon. As no ATLAS or CMS search shows a significant excess beyond the Standard Model expectation, mass limits have been set in various models. Figure 5 shows two interpretations within general gauge mediation models (GGM) models [68], with a bino-like or wino-like NLSP [69, 70] (GGM is a generalisation of GMSB models).

3.4 Simplified Models: Virtues and Challenges

In Sections 3.1 to 3.3, various results from SUSY searches have been interpreted in the context of so called “full models”. These are characterised by a relatively small number of parameters that fully specify the sparticle mass spectrum and thereby fix the production cross sections and branching ratios of every sparticle. In such models events can be in general realised in many different ways, e. g. by different primarily produced sparticles and by different combinations of the two decay chains. Although this provides realistic signatures for any assumed SUSY model with any set of specific parameters, the results are difficult to generalise to other models or event topologies. Another limitation is that in a given full model, the masses of different sparticles are often related in a way that can not be generalised. In the CMSSM, for example, there is the well known $\sim 1 : 2 : 6$ relation for $M_1 : M_2 : M_3$.

An alternative approach is the concept of simplified model searches (SMS) [71]: The basic assumption here is that only one particular event topology is realised, e.g. $pp \rightarrow \tilde{q}\tilde{q} \rightarrow q\tilde{\chi}_1^0 q\tilde{\chi}_1^0$. The only free parameters are then the masses of the two involved sparticles, namely $m_{\tilde{q}}$ and $m_{\tilde{\chi}_1^0}$, which make these “models” rather simple and easy to interpret. The production cross section is fixed by the squark mass [49], which potentially depends on the number of kinematically accessible squark flavours, as can be seen in figure 6.

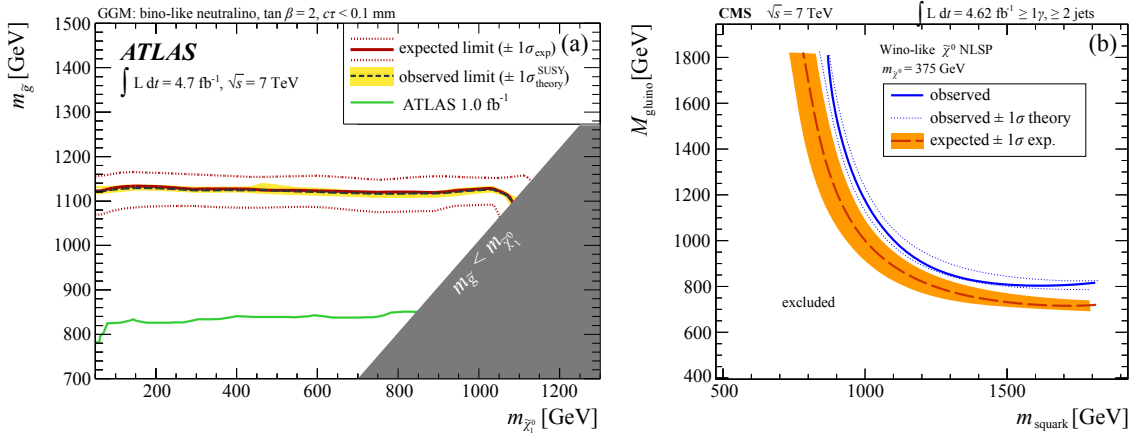


Fig. 5. Interpretation of the searches with photons, jets and $E_{\text{T}}^{\text{miss}}$ in the GGM. (a) Exclusion limit from a search with two photons in the plane spanned by the NLSP mass and the gluino mass for a bino-like NLSP. (b) Exclusion limit from a search with at least one photon in the plane spanned by the squark mass and the gluino mass for a fixed wino-like NLSP mass. (Adapted from Refs. [69, 70].)

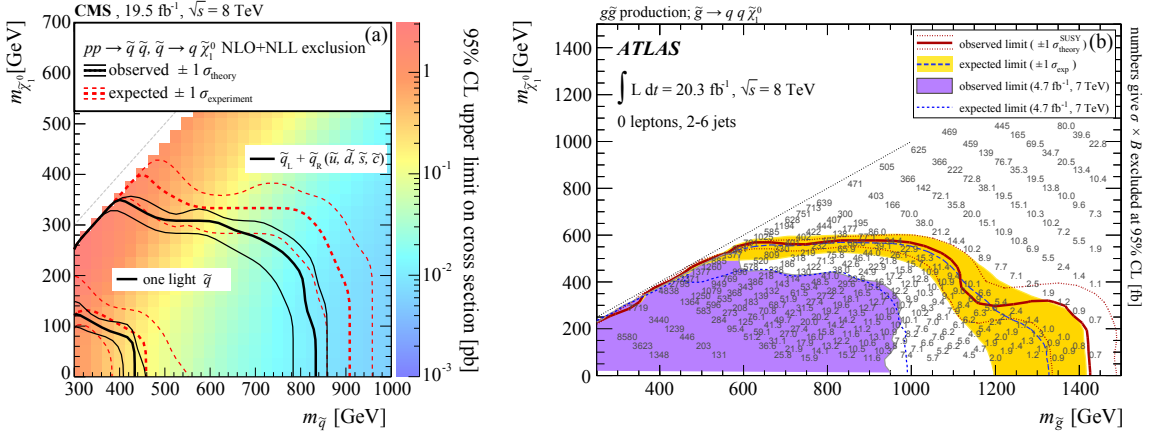


Fig. 6. (a) Interpretation of a CMS search with jets+ $E_{\text{T}}^{\text{miss}}$ in a simplified model with 100% branching ratio of $pp \rightarrow \tilde{q}\tilde{q} \rightarrow q\tilde{\chi}_1^0 q\tilde{\chi}_1^0$, with only one or four squark flavours kinematically accessible, shown in the $m(\tilde{q})$ - $m(\tilde{\chi}_1^0)$ plane. (b) A similar search by ATLAS interpreted in a simplified model with the decay topology $pp \rightarrow \tilde{g}\tilde{g} \rightarrow qq\tilde{\chi}_1^0\tilde{\chi}_1^0$ shown in the $m(\tilde{g})$ - $m(\tilde{\chi}_1^0)$ plane. (Adapted from Refs. [50, 51].)

With the data from Run 1, searches with jets and $E_{\text{T}}^{\text{miss}}$ are sensitive to gluino masses up to 1.3 TeV for events of the type $\tilde{g}\tilde{g} \rightarrow qq\tilde{\chi}_1^0\tilde{\chi}_1^0$, and squark masses up to 880 GeV for $\tilde{q}\tilde{q} \rightarrow qq\tilde{\chi}_1^0\tilde{\chi}_1^0$ (see figure 6).

Obviously, the assumption of a branching ratio of 100% in a particular final state leads to overly optimistic results if other final states with signatures that are difficult to find are realised for a significant fraction of the events. Therefore, the exclusion limit for a full model can only be achieved by the interpretation of the SMS result within this full model. An example for such an analysis is presented in section 6.1.

4 The Rest of the Spectrum: SUSY Searches for Electroweak and Third-Generation Production

In the previous section, searches for SUSY were discussed that aim at the most abundant signatures in generic implementations of SUSY. These generic signatures are also featured in the most common highly constrained models such as the CMSSM, where the mass scales of all sfermions are coupled to each other and all gauginos are coupled to each other. Thus, excluding high first-generation squark (and gluino) masses means that in models like the CMSSM also light sleptons and third-generation squarks and

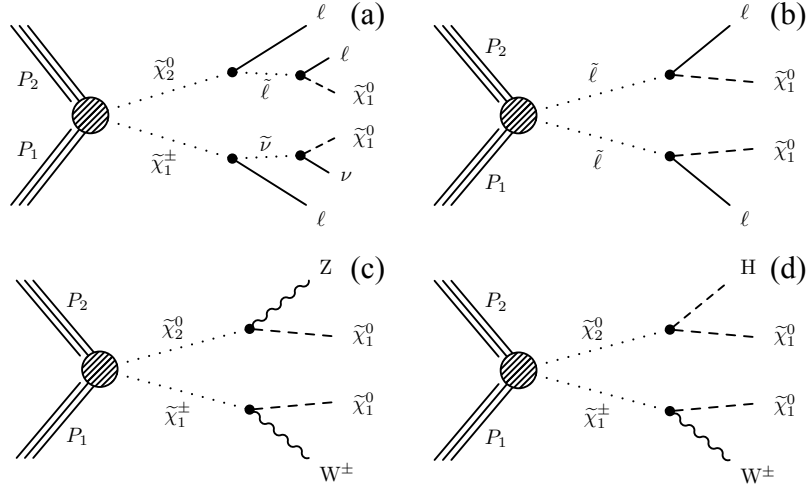


Fig. 7. Example diagrams for the production of gauginos or sleptons without the production of strongly interacting particles. These production processes involve electroweak interactions.

gauginos are indirectly excluded. In this section, searches are covered for which the simple assumption of maximally constrained SUSY shall not be a motivation.

The generic searches are motivated by the relatively high cross section of gluino production and first-generation and second-generation squark production, as shown in figure 1. However, as shown e.g. in figure 3, the limits obtained in this type of search in highly constrained SUSY models such as the CMSSM correspond to SUSY mass scales of gluinos and squarks of more than $M_{\tilde{g}} = 1.2$ TeV and $M_{\tilde{q}} = 1.8$ TeV, respectively. If all SUSY masses were that heavy, SUSY would cease to help the hierarchy problem, as discussed in section 3.

Therefore, in order to retain the feature of solving the hierarchy problem, it is theoretically attractive to think of more general SUSY models in which the mass scale of the sparticles that only interact weakly (the sleptons and gauginos) and the mass scale of the third-generation squarks are decoupled from the scale of the first-generation and second-generation squarks, and from that of the gluinos. It is easily possible to realise such a model in the framework of the MSSM or in even more general models. On the other hand, there is no obvious choice for a benchmark model for such a scenario, defined at the GUT scale with only a very small number of parameters. This is in contrast to the generic searches. Thus, the results of the specific searches for SUSY in electroweak production processes or in the production of third-generation squarks ask for a more model-independent parametrisation, to allow for the later interpretation of the search results in any specific SUSY model. This is mostly realised in the form of the so-called simplified model searches already introduced in the previous section. While this section covers the searches and the translation of their results into SMS limits, the application of these limits is discussed further in section 6.1.

4.1 Electroweak Production of SUSY Particles

Searches for SUSY events with electroweak interactions at the production vertex can be classified in two different ways: first, by the type of SUSY particles occurring at the production vertex, and second, by the visible final-state particles. Examples for production and decay processes are shown in figure 7.

It can be seen that some of the fundamental features of SUSY events already discussed in section 3 are retained: Leptons in the final state allow events to be distinguished from the QCD background, and in R -parity conserving models missing transverse energy E_T^{miss} is produced by the escaping LSPs, here assumed to be the lightest neutralinos $\tilde{\chi}_1^0$. However, there are also significant differences with respect to generic searches for SUSY events involving the strong interaction at the production vertex: There, the high production cross section of up to $\mathcal{O}(10$ pb) (depending on the mass scale, see figure 1) made possible by the strong interaction allows rather heavy SUSY objects to be produced at the 8 TeV LHC Run 1. However, in electroweak production processes for SUSY particles not interacting strongly, there is a reduction in the production cross section at the same mass scale of more than a factor of 100.

Thus, at the same centre-of-mass energy, the accessible mass scales for the direct production of sleptons and gauginos is significantly lower than for first-generation squarks and gluinos. Consequently, also the transverse momenta of the final-state particles and the expected E_T^{miss} are significantly lower than for strong-production processes of heavy squarks and gluinos—a fact that can limit the selective power of the trigger and the offline selection.

While gauginos couple directly to the quarks in the protons via gauge interactions, the sleptons need an intermediate SM gauge boson to couple to the partons in the beam protons. This explains why the direct production of sleptons again is suppressed with respect to the gaugino production by about a factor of 100.

As shown in figure 7, different production modes can yield very similar final states. Leptonic decays of W and Z bosons are employed, which means that the first three diagrams yield near-identical final-state particle compositions of two or more leptons and missing energy. Depending on the intermediate particles, the expected kinematics may vary. On the other hand, the usable decays of Higgs bosons, e.g. into b quarks, τ leptons or two photons, yield final states with two hadronic heavy quark jets or two photons. Therefore, a strategy is employed where the searches are classified by final-state particles, and each search can then be interpreted in simplified models describing different production mechanisms, which can be optimally constrained by an individual final state. In the following, out of a very large number of available searches [62, 72–77], the following examples are discussed in detail: the production of 2-lepton and 3-lepton final states in conjunction with E_T^{miss} , where the leptons can be electrons or muons; the production of τ -lepton final states with E_T^{miss} ; and the specific search for SUSY decays with electroweak production of SUSY particles with a Higgs boson in the decay chain.

The first example discussed here stems from ATLAS and CMS searches for 2 or 3 leptons and E_T^{miss} , where the leptons can come in same-sign or opposite-sign configurations [73, 76]. It can be beneficial to also search for same-sign lepton configurations in cases where one out of three leptons is outside of the detector acceptance in production processes as shown in figure 7(a). The dominant background to these searches are diboson events (W^+W^- , $W^\pm Z$ and ZZ), W^\pm +jets and Z +jets events, and $t\bar{t}$ production with a small contamination of leptons from secondary decays, e.g. from heavy quarks.

Examples for discriminating variables employed in these searches are given in figure 8. An example for a signal region aiming at SUSY decays involving two W^\pm bosons is shown in figure 8(a) from the ATLAS experiment. The plot shows the distribution of the invariant mass of two opposite-sign same-flavour (SF) leptons $m_{\ell\ell}$, where $\ell = e, \mu$.

An example of another signal region is shown in figure 8(b). It exploits the “stransverse” mass m_{T2} for two leptons of different flavours (DF) [56, 57], defined as

$$m_{T2} = \min_{\mathbf{q}_T} \left[\max \left(m_T(p_{T,\ell 1}, \mathbf{q}_T), m_T(p_{T,\ell 2}, p_T^{\text{miss}} - \mathbf{q}_T) \right) \right],$$

where $p_{T,\ell 1}$ and $p_{T,\ell 2}$ are the transverse momenta of the two leptons, and \mathbf{q}_T is a transverse vector that minimises the larger of the two transverse masses m_T . The latter is defined by

$$m_T(\mathbf{p}_T, \mathbf{q}_T) = \sqrt{2(p_T q_T - \mathbf{p}_T \cdot \mathbf{q}_T)}.$$

For SM $t\bar{t}$ and W^+W^- events, in which two W^\pm bosons decay leptonically and p_T^{miss} originates from the two neutrinos, the m_{T2} distribution has an upper end-point at the W^\pm mass. For signal events, the undetected LSP contributes to p_T^{miss} , and the m_{T2} end-point is correlated to the mass difference between the slepton or chargino and the lightest neutralino. For large values of this difference, the m_{T2} distribution for signal events extends significantly beyond the distributions obtained from $t\bar{t}$ and W^+W^- events. This is clearly visible in figure 8(b), where the background drops strongly on the logarithmic scale at about $m_{T2} \approx M_W$, while the signal stays flat.

Other typical observables besides the leptonic invariant mass, m_{T2} and m_T , are H_T (see section 3.1), E_T^{miss} and $m_{\text{eff}} = H_T + E_T^{\text{miss}}$. Examples for E_T^{miss} are given in figure 8(c,d), for the signal regions aimed at decays via W^\pm and Z (c) and for decays of the gauginos via staus (d). The latter is favourable in many models motivated by the stau co-annihilation mechanism of reducing the predicted amount of dark matter in the universe down to the measured values (see section 6.1). There, the stau is the NLSP and thus is kinematically favoured in the decay of heavier SUSY particles. It can be seen that the SM backgrounds drop strongly for growing E_T^{miss} , and only SM processes with true E_T^{miss} from e.g. $Z \rightarrow \nu\bar{\nu}$ decays remain at large values. On the other hand, due to the energy carried by the LSP, SUSY processes on average show much higher E_T^{miss} values compared to the background. Thus, high signal-to-background ratios can be reached at very high E_T^{miss} .

Neither ATLAS nor CMS observed a significant SUSY signal in any of these signal regions in Run 1. Thus, the results of the searches are converted into limits on SMS decay chains, as already discussed in

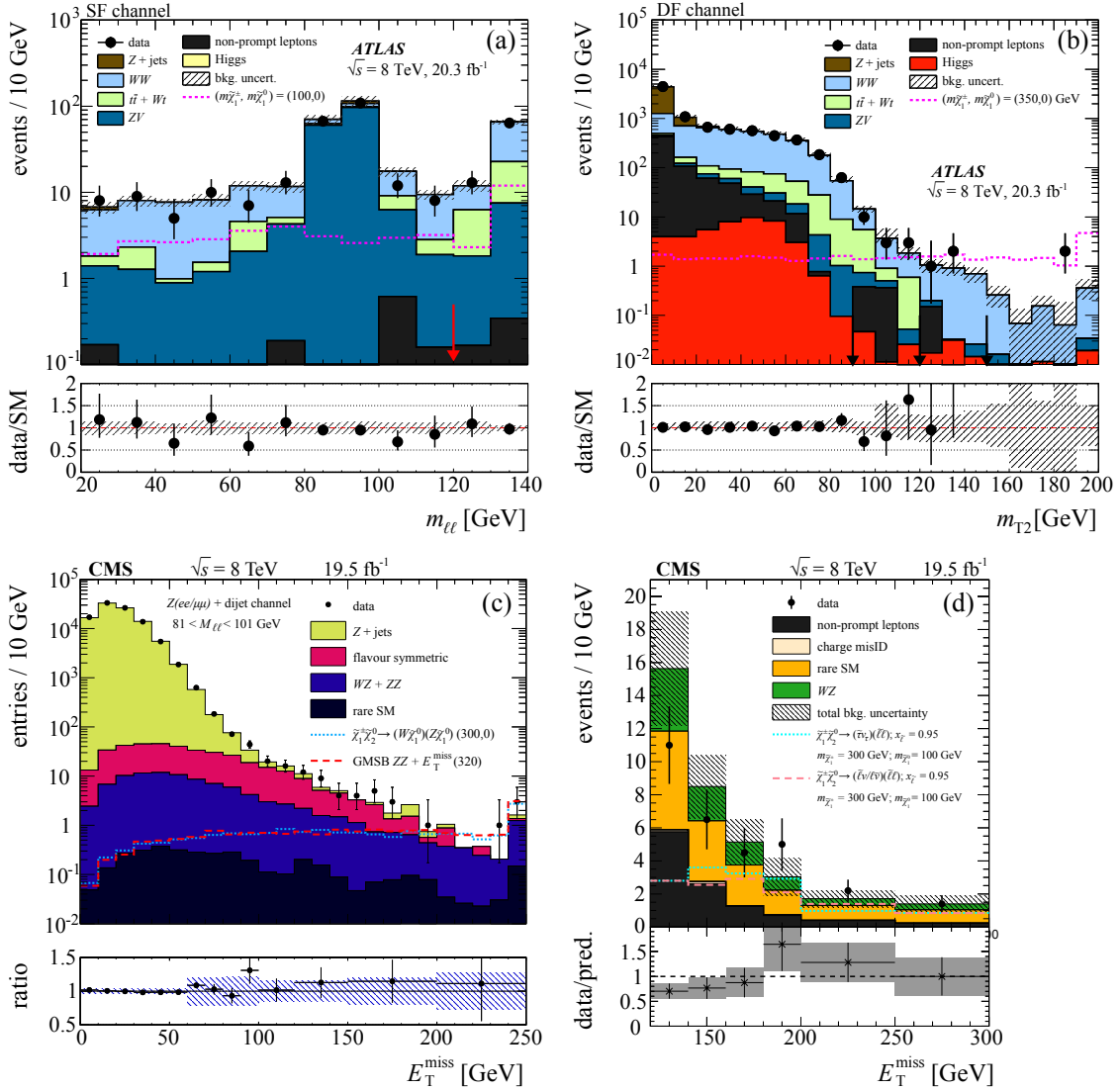


Fig. 8. Selected observables from the searches for the production of gauginos and sleptons via the electroweak interaction from ATLAS (a,b) and CMS (c,d). See the text for a discussion of the observables, signal properties and backgrounds. (Adapted from Refs. [73, 76]).

section 3.4. Since different signal regions can be sensitive to different signals depending on the kinematical configuration, expected limits from all signal regions are derived for all model points and decay chains. The observed limit for a given decay chain and model point is then calculated only for the signal region with the strongest expected limit.

Examples for the limits derived for the searches described above are given in figure 9. The top row shows examples from the ATLAS experiment, the bottom row from the CMS experiment. The considered SMS decay chains are $\tilde{\chi}_1^+ \tilde{\chi}_1^- \rightarrow \tilde{\ell}\nu/\tilde{\nu}\ell \rightarrow 2\ell\nu\tilde{\chi}_1^0$ with $m_{\tilde{\ell},\tilde{\nu}} = (m_{\tilde{\chi}_1^\pm} - m_{\tilde{\chi}_1^0})/2$ (figure 9(a)), $\tilde{\ell}^+\tilde{\ell}^- \rightarrow 2\ell^\pm\tilde{\chi}_1^0$ (b), $\tilde{\chi}_2^0\tilde{\chi}_1^\pm \rightarrow Z\tilde{\chi}_1^0W\tilde{\chi}_1^0$ (c), and $\tilde{\chi}_2^0\tilde{\chi}_1^\pm \rightarrow h\tilde{\chi}_1^0W\tilde{\chi}_1^0$ (d). The physical masses of the SUSY particles involved are given on the axes of the plots, while the numbers (ATLAS) respectively color scale (CMS) give the cross section of the exclusive production of the decay chain under investigation that can be excluded at the 95% CL. If only two SUSY masses are involved, this limit on the cross section of individual decay chains can be interpreted directly in every SUSY model which involves the decay chain, as long as there is no strong dependence on the production process. It is possible that—depending on the nature of the gauginos in a given physical model—the relative strengths of the predicted s -channel and t -channel production processes do vary, which could influence the selection efficiency and thus the limit on the cross section. Therefore, in some cases t -channel production is removed from the simulated process by assuming the

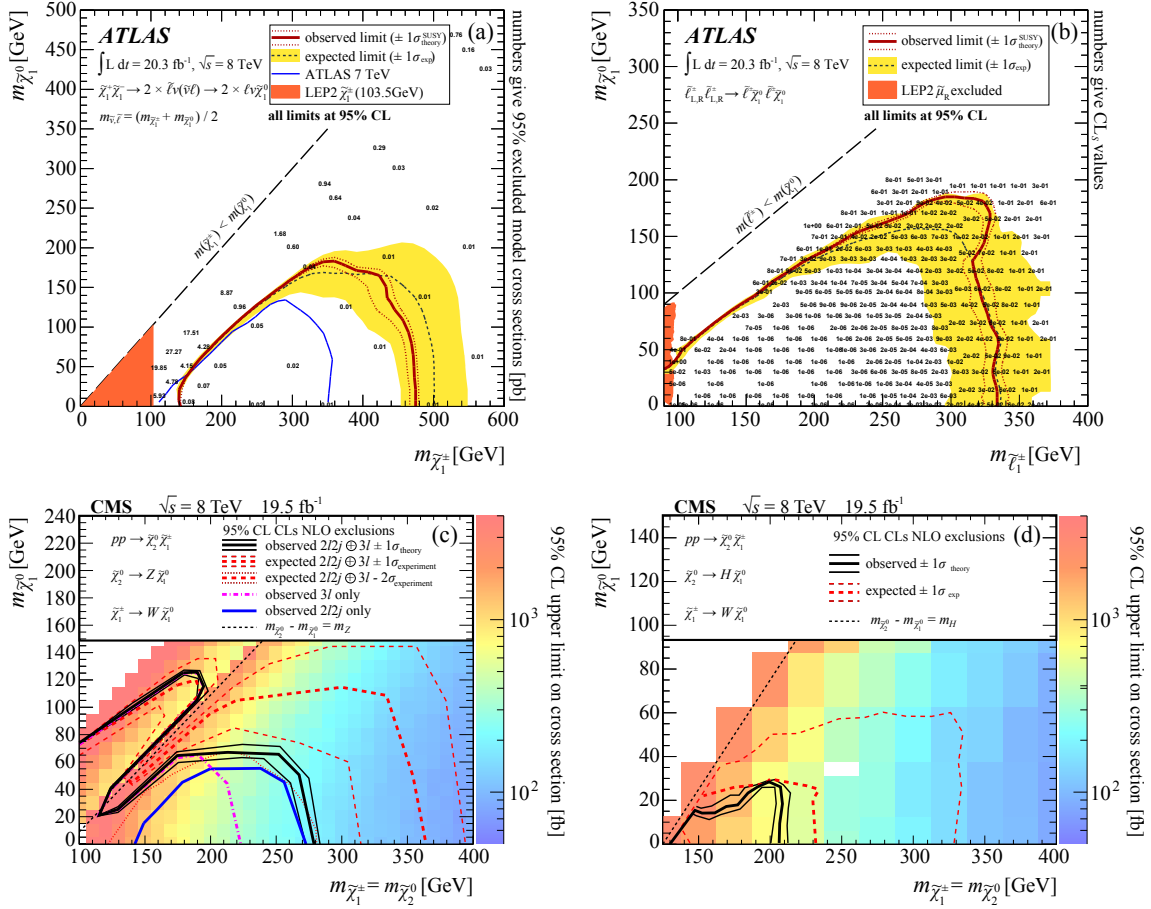


Fig. 9. The resulting limits on selected SMS decay chains from ATLAS (a,b) and CMS (c,d). The excluded production cross section of the decay chain given in the figures is plotted against the masses of the physical SUSY particles appearing in the decay chain. The expected exclusion lines in the plots are given by the assumption of the full electroweak coupling at the production and of 100% branching fractions into the studied final state. Individual kinematical assumptions on the particles involved in the decay are also given in the plots. (*Adapted from Refs. [73, 76].*)

particle in the t -channel, e.g. a squark in the SMS implementation, to be very heavy. However, influences from differences in the production process for the same decay chains are typically weak.

A more challenging situation arises for decay chains with more than two different SUSY particles that are not degenerate in mass. One example is the decay chain $\tilde{\chi}_1^+ \tilde{\chi}_1^- \rightarrow \tilde{\ell} \nu / \tilde{\nu} \ell \rightarrow 2 \ell \nu \tilde{\chi}_1^0$ decay chain in figure 9(a) with the explicit assumption of $m_{\tilde{\ell}, \tilde{\nu}} = (m_{\tilde{\chi}_1^\pm} - m_{\tilde{\chi}_1^0})/2$. Also this latter condition has an effect on the acceptance and efficiency of the search. However, this assumption is not generically true in all physical models to which the SMS limit shall be applied. Thus, the correct interpretation of such limits might involve additional studies of changes in the detector acceptance between SMS implementation and physical model.

A general feature of the limits is that, for specific mass relations, the momenta of the visible decay products become small. For the decay chains that proceed via the emission of SM fermions with negligible mass (see figure 9(a,b)), this is the case for $m_{\tilde{\chi}_1^\pm} = m_{\tilde{\chi}_1^0}$ or $m_{\tilde{\ell}} = m_{\tilde{\chi}_1^0}$, respectively. For the cases of figure 9(c,d), where heavy SM gauge bosons are emitted from the decay chain, the kinematical condition in which the sensitivity vanishes changes to $m_{\tilde{\chi}_1^\pm} - m_{\tilde{\chi}_1^0} = m_{V,H}$. In these cases, the trigger and selection efficiencies degrade considerably, leading to a very weak exclusion. This is one of the two reasons why—unfortunately—no general statement in the form of “gauginos (or sleptons) are excluded up to a mass of” can be derived from the LHC search results.

The other reason for the lack of universal limits on individual SUSY production modes can be exemplified as follows: Figure 10 shows the interpretation of leptonic searches with three leptons (e, μ or τ) [72]. Assuming an exclusive branching ratio of $\tilde{\chi}_2^0 \rightarrow Z + \tilde{\chi}_1^0$ (figure 10(a)) is neglecting a possibly

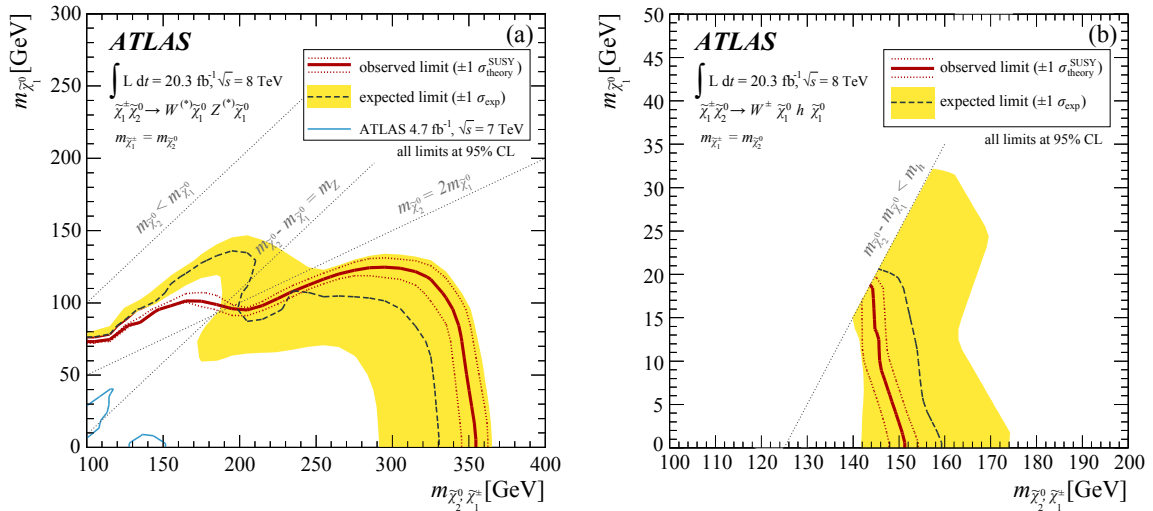


Fig. 10. Interpretation of ATLAS searches in final states with three leptons (e , μ or τ) for direct chargino and neutralino production. As expected, the limits on the sparticle masses for an assumed simplified model with $\tilde{\chi}_2^0 \rightarrow Z + \tilde{\chi}_1^0$ (a) are much stronger than those for the case of decay chains involving the SM-like Higgs boson h : $\tilde{\chi}_2^0 \rightarrow h + \tilde{\chi}_1^0$ (b). (Adapted from Ref. [72].)

large branching ratio including a SM-like Higgs boson h in the form of $\tilde{\chi}_2^0 \rightarrow h + \tilde{\chi}_1^0$ (figure 10(b)). Both can yield the same final state, however with strongly different SM branching fractions to the visible final-state particles and with different yields of τ leptons versus light leptons. In a physical model, the real limit would have to be derived for a combination of the two decay channels given above. Since the limits derived for the two channels differ significantly due to the much weaker branching fraction of the Higgs boson into light leptons, the limit has to be evaluated for each model point depending on its individual prediction for the branching fractions.

Many other interesting search channels are covered along the lines described above by the ATLAS and CMS experiments. Examples are the search for electroweak SUSY production with τ leptons without accompanying jets [75, 76] or more specific searches with Higgs bosons in the decay chain [78].

A summary of CMS searches for electroweak production of gauginos is given in figure 11 [76, 77]. Similar results are available from ATLAS [72, 73, 75]. Depending on which particles are involved, different kinematical bounds exist. The strongest limits in terms of the accessible mass range are obtained for $\tilde{\chi}_1^\pm \tilde{\chi}_2^0 \rightarrow \tilde{\ell} \nu / \tilde{\ell} \ell \rightarrow 3\ell \nu 2\tilde{\chi}_1^0$ in specific 3-lepton searches [72, 76] that show a very striking signature of 3 light leptons with high transverse momenta and large E_T^{miss} . For both ATLAS and CMS, masses of up to $m_{\tilde{\chi}_1^\pm} = m_{\tilde{\chi}_2^0} \approx 700$ GeV can be excluded at the 95% CL. However, for small values of $m_{\tilde{\chi}_1^\pm} - m_{\tilde{\chi}_1^0}$, the visible momenta of the leptons disappear. Thus, even for an assumption of an exclusive branching fraction in the given decay mode and full electroweak coupling strength at the vertex, $m_{\tilde{\chi}_1^\pm} \approx m_{\tilde{\chi}_2^0} \approx 200$ GeV is still allowed. In many SUSY breaking scenarios, however, some fine-tuning of the parameters is needed in order to achieve $m_{\tilde{\chi}_1^\pm} \approx m_{\tilde{\chi}_1^0}$.

4.2 Searches for SUSY Particles of the Third Generation

As already motivated in section 2, there is a strong interest in the third-generation squarks. The main reason for this is twofold: First, third-generation squarks play a key role in determining the mass of the SM-like Higgs boson h in a SUSY model. If their mixing is large, i.e. if large mass splittings between the different mass eigenstates \tilde{t}_1 and \tilde{t}_2 (or between \tilde{b}_1 and \tilde{b}_2) occur, then $m_h \approx 126$ GeV can be achieved without excessively unnatural mass hierarchies between the SUSY particles and their SM partners. Furthermore, the large mass splitting yields a situation where \tilde{t}_1 and \tilde{b}_1 are the lightest predicted squarks. Second, the production cross section of third-generation squarks at the LHC is about one order of magnitude lower than the corresponding cross sections of the SUSY partners of light quarks at the same mass (see figure 1), despite sharing the same couplings. This is a consequence of the negligible heavy-quark content of the proton. Therefore, $\tilde{t}_{1,2}$ and $\tilde{b}_{1,2}$ can only be produced in s -channel processes via a gluon, and not in the s -channel via a quark or in t -channel processes. While the discovery of $\tilde{t}_{1,2}$ and $\tilde{b}_{1,2}$ thus

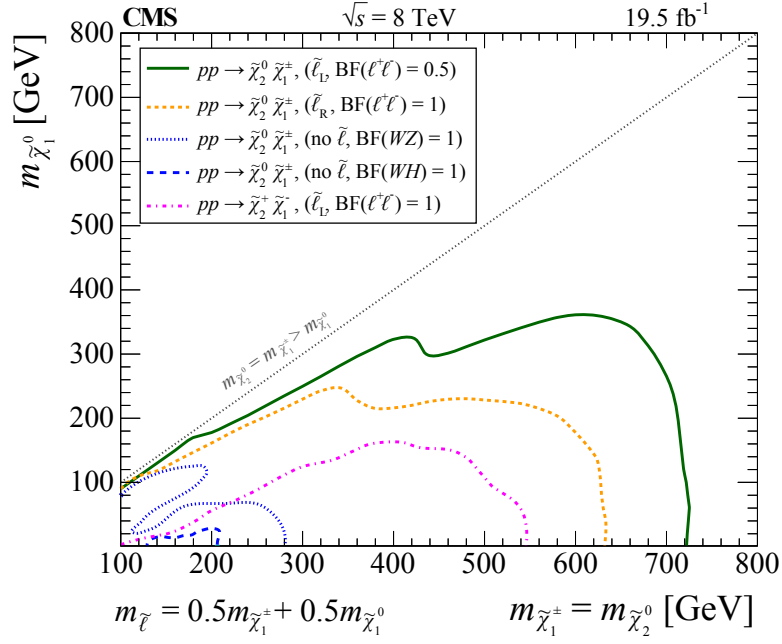


Fig. 11. Overview plot of a selection of published limits on gaugino production from the CMS collaboration. All limits are given in the form of SMS limits on individual production processes. Similar results are available from the ATLAS collaboration. (*Adapted from Ref. [76].*)

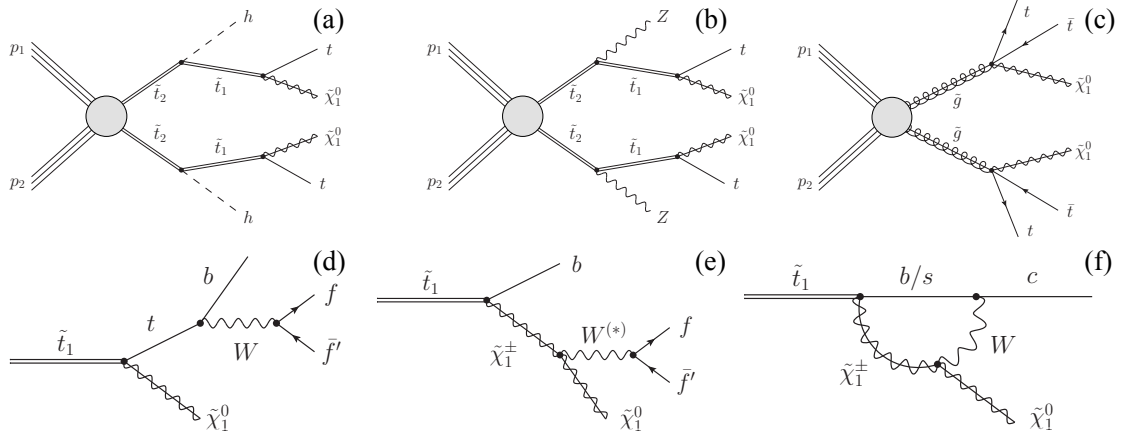


Fig. 12. Example diagrams for the production and decay of top quarks in conjunction with the production of the lighter or heavier stops or gluinos.

would be of highest importance in the context of the connection between SUSY and the Higgs sector, their lower cross section makes them more difficult to pin down than the more abundantly produced first-generation squarks.

Figure 12 shows the typical production and decay processes of stops. They can either be produced directly as the heavier mass eigenstate with a decay via a Higgs boson (a) and via Z bosons (b), or via the decay of gluinos (an example for a three-body-decay of a gluino with a virtual stop is given in (c)). Further, if the lighter mass eigenstate is produced, its decay could proceed via neutralinos (d) or charginos (e,f). Therefore, a complex collection of different final states can be searched for, the realisation of which depends both on the couplings of the model and on the kinematical configuration.

These kinematical configurations are shown in figure 13 in the $m_{\tilde{t}_1} - m_{\tilde{\chi}_1^0}$ plane. For large $m_{\tilde{t}_1}$, the direct two-body decay $\tilde{t}_1 \rightarrow t\tilde{\chi}_1^0$ is open. For very large $m_{\tilde{t}_1}$, the top quark from the decay is boosted strongly in the transverse direction, which might require specific reconstruction techniques, as outlined

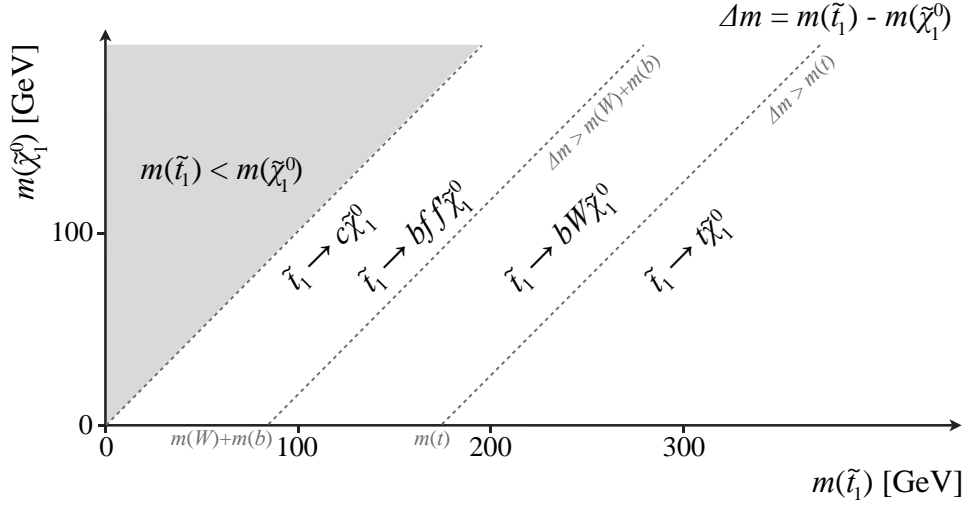


Fig. 13. A schematic illustration of the different kinematical areas which determine the selection topology of stop searches. (Adapted from Ref. [79].)

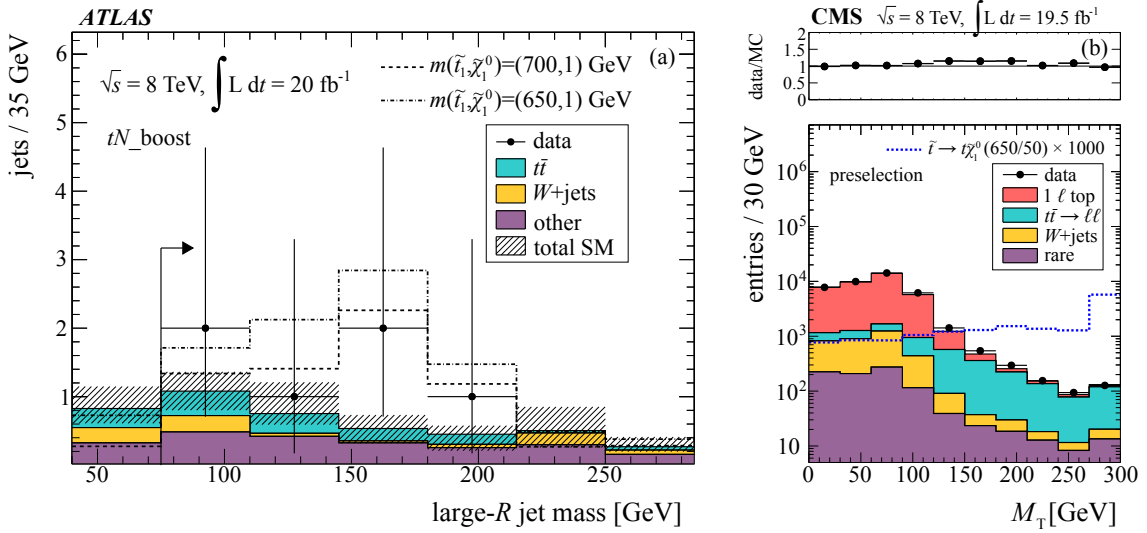


Fig. 14. Illustrations of typical selection variables for searches for \tilde{t}_1 decays. (a) The ATLAS search for heavy stops yielding fat jets shown in the form of the jet mass of the fat jet. (b) An example from CMS with a search for intermediate-mass stops shown in the form of the transverse-mass distribution. (Adapted from Refs. [79, 80])

below. As soon as $m_{\tilde{t}_1} - m_{\tilde{\chi}_1^0} = m_t$ is reached, the direct two-body decay is closed and the sensitivity drops to zero. For smaller $m_{\tilde{t}_1}$, the decay via a (virtual) chargino into the same final state can be used: $\tilde{t}_1 \rightarrow b\tilde{\chi}_1^\pm \rightarrow bW^\pm\tilde{\chi}_1^1$. For $m_{\tilde{t}_1} - m_{\tilde{\chi}_1^0} = m_b + M_{W^\pm}$, also this channel closes and the sensitivity vanishes again. Then, the decay via virtual $W \rightarrow ff'$ or the decay $\tilde{t}_1 \rightarrow c\tilde{\chi}_1^0$ remains. Finally, the region $m_{\tilde{t}_1} < m_{\tilde{\chi}_1^0}$ is uninteresting from a cosmological point of view.

Out of a very large set of available searches [78–87], a few examples shall be explained in the following. Figure 14 shows examples from the event selections of such searches. For the ATLAS experiment, an example from a search for heavy stops is shown [79]. For large $m_{\tilde{t}_1} \gg m_t + m_{\tilde{\chi}_1^0}$, the top quark from the decay and the hadronic decay products of the $t \rightarrow bW \rightarrow bff'$ decay are strongly boosted, and the top quark cannot easily be reconstructed from the individual jets of its decay products. In this case, the search for so-called “fat jets” or “large- R jets” is employed. First, an anti- k_t jet with a very wide radius parameter $R = 1.0$, $p_T > 150$ GeV and $|\eta| < 2.0$ is reconstructed [88, 89]. Within this jet, jet trimming [90] is applied with an anti- k_t jet finder and $R = 0.3$. From all objects within the large- R jets

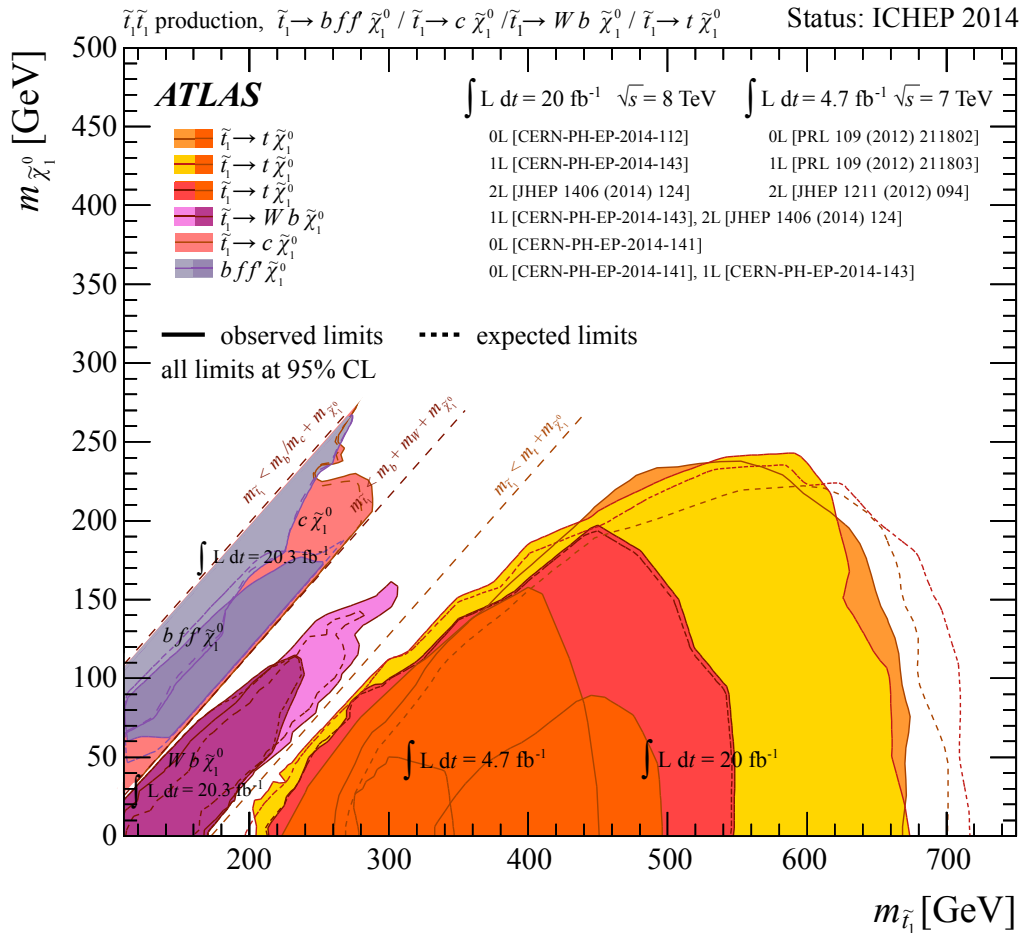


Fig. 15. A selection of published limits on the production of third-generation squarks from the ATLAS experiment. All limits are given in the form of SMS limits on individual production processes (see references in the plot). Similar results are obtained from the CMS experiment (see e.g. Ref. [80]). (Adapted from Refs. [79, 82, 84, 87, 91–93].)

that carry a fraction of more than 0.05 of the transverse momentum of the large- R jet, an invariant mass is reconstructed. The distribution of this reconstructed mass is shown in figure 14(a) after preselection cuts. Flavour tagging is then applied to the sub-jets, which should contain a b -quark jet. It can be seen that for signal events, the jet-mass distribution shows a very broad peak-like structure around the top-quark mass. The remaining backgrounds are $t\bar{t}$ and single top quark production, $t\bar{t}$ production in association with a vector boson, Z +jets, and diboson production. The data show a slight, but insignificant excess over the background.

An example is a search from the CMS experiment, which is both sensitive to $\tilde{t}_1 \rightarrow t\tilde{\chi}_1^0$ and to non-resonant $\tilde{t}_1 \rightarrow bW\tilde{\chi}_1^0$ at intermediate values of $m_{\tilde{t}_1}$ [80]. There, the variable m_T already introduced in the previous section is used as a discriminator against events where the real missing transverse energy is exclusively stemming from a $W \rightarrow \ell\nu$ decay, such as semileptonic $t\bar{t}$ events. No excess over the background is observed, and the variable is used as an input to a multivariate selection, from which limits are derived.

An overview of the currently published search results and limits is given in figure 15 using examples from the ATLAS collaboration [79, 82, 84, 87, 91–93]. Similar results are available from CMS [80]. As expected, the observed sensitivity is governed by the kinematic regions defined in figure 13. The strongest limits reach up to $m_{\tilde{t}_1} > 700$ GeV for the assumption of the full strong-production cross section and, more importantly, of 100% branching ratio into the given decay. This limit by itself is already touching the areas which could be considered theoretically interesting for an elaboration on the natural ability of SUSY to explain the hierarchy problem of the SM, without unduly fine-tuning the SUSY-parameters themselves. For $m_{\tilde{t}_1} \approx \mathcal{O}(1 \text{ TeV})$ and higher, the difference between the SUSY scale and the electroweak scale becomes too large to explain the hierarchy problem of the SM Higgs mass without additional assumptions. However, as explained in section 4.1, the kinematics of the decays close to the

kinematic transitions leads to vanishing momenta of the visible final-state SM particles, which in turn yields vanishing exclusions. Therefore, it remains for a global analysis in a given model to look for candidates of SUSY implementations which are still in agreement with the allowed low stop and low neutralino masses. An example of such an analysis is shown in section 6.1.

5 Exotic SUSY Scenarios

The searches for SUSY described in the previous sections are motivated by models with a wide range of assumptions. These range from cosmological constraints (like a neutral stable LSP) over flavour physics precision measurements (no additional tree-level FCNC) to aesthetic arguments (fine-tuning). However, none of these are strictly required to be applicable for a realistic SUSY scenario. For example, the dark matter in the universe could be explained by something entirely unrelated to SUSY, while SUSY still could explain electroweak symmetry breaking and the mass scale of the Higgs boson. It is the aim of this section to introduce a brief selection of searches in which the motivation goes beyond the most constraint and most beautiful SUSY models.

The first part of this section deals with charged long-lived heavy SUSY particles. The focus of the second part lies on what happens if the explanation of the dark matter in the universe is omitted from the motivation of SUSY. The last part covers scenarios with compressed mass spectra, i.e. scenarios in which the mass difference between the initially produced SUSY particle and the sum of the decay products is small. Such scenarios lead to final states with only soft particles and thus to challenging signatures.

5.1 Searches for Long-Lived SUSY Particles

Long-lived SUSY particles can have various origins. They can occur in models with a very small mass difference between a charged NLSP and the neutral LSP, in which case the Lorentz-invariant phase-space volume is small. Such scenarios can be realised, for example, in the pMSSM when the parameter M_2 is much smaller than M_1 and μ . Then, the NLSP and the LSP are wino-like and both have a mass close to M_2 . Similarly, the mass difference can become small when μ is small compared to M_1 and M_2 , but then it is typically a bit larger than in the first case. Searches for heavy stable charged particles, which are causing large energy deposits in the tracking detectors, can be reinterpreted in SUSY models like the ones mentioned, but this is beyond the scope of this review.

Another potential origin for long-lived SUSY particles are scenarios with a small coupling of the NLSP to the LSP. Such a situation can come about because of a small coupling constant itself, as in the case of GMSB models where the LSP is the gravitino which couples very weakly to the NLSP. Alternatively, the coupling can be small because of heavy virtual particles in the decay process. One scenario for this is “split SUSY” [42, 43] (see section 2.2), where the gluino and the other gauginos might be accessible at the LHC, but all scalar SUSY particles are very heavy. Since the decay of the gluino can only happen via squarks, it is much suppressed, and the gluino lifetime is long. The gluino is then forming a colour-singlet state, a so-called R -hadron, which can pass through the detector and might be stopped by hadronic interactions in one of the detector components, most likely in the dense calorimeter material. Then, after some time, the stopped gluino will decay, providing a distinct signature of hadronic activity in the calorimeter without associated tracks pointing to the interaction point. This also happens in time intervals with no bunch crossings which allows such events to be triggered with low thresholds on the energy deposit in the hadronic calorimeter [94, 95]. Using this technique, gluino masses up to 830 GeV can be excluded for a generic R -hadron model with gluino lifetimes between 10^{-6} and 10^4 seconds.

For models with intermediate lifetimes of the NLSP, it may not reach the outer parts of the detector, but decay inside it. A possible scenario for such meta-stable particles would be a chargino with the decay $\tilde{\chi}_1^\pm \rightarrow W^*(\rightarrow ff')\tilde{\chi}_1^0$. Since here the mass difference between LSP and NLSP is small, the momenta of the visible decay products are very soft and might not be detectable. However, if the lifetime is long enough for the chargino to travel at least through some fraction of the inner tracking detectors, the signature of a disappearing track provides sensitivity to such models. So far, no excess of events with disappearing tracks has been observed at ATLAS or CMS, and a lower limit on the mass of meta-stable charginos has been set at 270 GeV in one particular SUSY model [96].

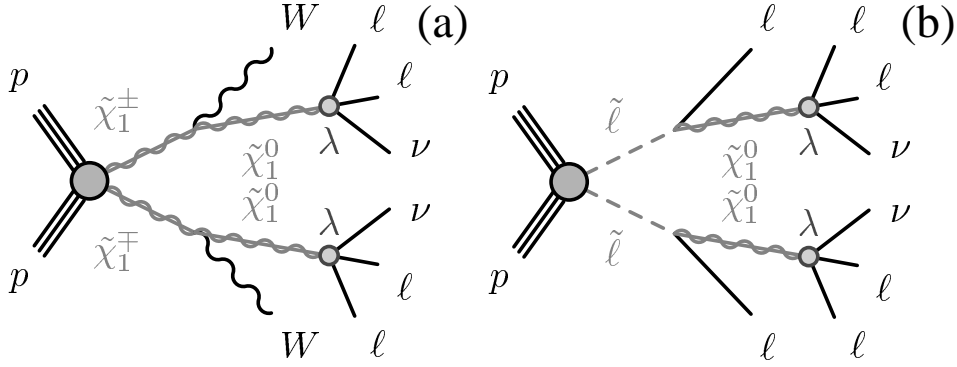


Fig. 16. Representative diagrams of SUSY final states in models with R -parity-violating SUSY and leptonic R -parity-violating couplings. (a) chargino NLSP; (b) slepton NLSP.

5.2 Searches for R -Parity-Violating Models

In generic SUSY models with minimal particle content, the SUSY Lagrangian includes terms that violate conservation of lepton (L) and baryon (B) number [97, 98], e.g.

$$\frac{1}{2}\lambda_{ijk}L_iL_j\bar{E}_k + \lambda'_{ijk}L_iQ_j\bar{D}_k + \frac{1}{2}\lambda''_{ijk}\bar{U}_i\bar{D}_j\bar{D}_k,$$

where L_i and Q_i indicate the lepton and quark $SU(2)$ -doublet superfields, respectively, while \bar{E}_i , \bar{U}_i and \bar{D}_i are the corresponding singlet superfields. The indices i, j and k refer to quark and lepton generations. The Higgs $SU(2)$ -doublet superfield H_2 is the Higgs field that couples to up-type quarks. The λ_{ijk} , λ'_{ijk} and λ''_{ijk} parameters are new Yukawa couplings.

Since the superfields contain both SM particles and SUSY particles, they e.g. couple two SM particles to only one SUSY particle. This means that, generally, single SUSY particles can be produced, and they can decay into final states where only SM particles are present.

In the absence of a protective symmetry, L - and B -violating terms may allow proton decay at a rate that is in conflict with the tight experimental constraints on the proton's lifetime [99]. This difficulty can be avoided by imposing the conservation of R -parity defined as $P_R = (-1)^{3(B-L)+2S}$ as introduced in section 2.1. However, experimental bounds on proton decay can also be evaded in R -parity-violating (RPV) scenarios, as long as the Lagrangian conserves either L or B , because then one of the two steps of the proton decay remains forbidden: either the production of a single SUSY particle from an up- and a down-quark in the proton, or the decay of the SUSY particle into light SM particles, such as leptons and a pion or kaon. Since in RPV models, single SUSY particles can decay, it means that in such a model there is no stable LSP, and thus no SUSY candidate for dark matter.

Therefore, an obvious way to generate an interesting search scenario at the LHC that does not contradict proton-lifetime bounds is to just allow non-zero values of λ_{ijk} . Then, B remains conserved and only L can be violated. The SUSY LSP decays into leptons, generating spectacular signatures consisting of a large number of isolated charged leptons and E_T^{miss} only from the neutrinos. A search along these lines for final states with at least four isolated leptons, including electrons, muons and τ leptons, was performed by the ATLAS experiment [74]. Examples for processes leading to such final states are shown in figure 16.

The signal regions selected for such a search are defined by only 3 conditions: First, at least four light leptons or τ leptons are required; second, a moderate requirement on $E_T^{\text{miss}} > 50$ GeV is imposed; and third a veto against the Z resonance on same-flavour opposite-sign leptons is applied. The veto is applied because the typical SM backgrounds are rich in Z bosons, such as WZ , ZZ , Z +jets and rare processes such as ZWW , ZZW and $t\bar{t}Z$. No significant excess of the data over the background is observed, and thus limits are set on the allowed cross section at the 95% CL in SMS scenarios, e.g. on topologies defined by the processes depicted in figure 16. Assuming the couplings in the SMS scenario and 100% branching ratio in the final state under study (which, again, is typically not true in any physical model), mass limits on the NLSP and the LSP can be set. As an example, for a chargino NLSP up to $m_{\tilde{\chi}_1^\pm} > 750$ GeV can be excluded for exclusive decays into light leptons, and $m_{\tilde{\chi}_1^\pm} > 550$ GeV for decays involving τ leptons, which allow significantly higher backgrounds from QCD jets than light leptons. In these searches, the

limit does not vanish for degenerate masses (as in the searches presented in section 4), because for RPV decays the search does not depend heavily on the particles emitted between the NLSP and the LSP. Instead, the sensitivity vanishes for $m_{LSP} \rightarrow 0$ GeV, because then the LSP is highly boosted and its decay products are collinear and cannot be individually reconstructed anymore.

5.3 Compressed Spectra

In scenarios where the mass difference of the initially produced SUSY particle and the sum of the decay products is small, like e.g. in the case of compressed SUSY [100], the transverse momentum of the final-state objects is in general small. It is, consequently, very challenging to trigger and select signal events from such models, although—e.g. in the case of gluino or squark production—the production cross section might be very large. One possibility to get some sensitivity to such models is similar to the search at colliders for direct Dark Matter production: Initial-state or final-state radiation with high transverse momentum is leading to mono-jet or mono-photon signatures, or to signatures with only one W/Z boson. A reinterpretation of these searches in SUSY scenarios provides some sensitivity to compressed mass spectra.

One example is a search for light \tilde{t}_1 which are almost mass-degenerate with the $\tilde{\chi}_1^0$ [87]. For such a scenario, the decay via virtual $W^* \rightarrow ff'$ or the CKM-suppressed decay $\tilde{t}_1 \rightarrow c\tilde{\chi}_1^0$ are possible (see section 4.2 for details). In the latter case the sensitivity can be further improved by distinguishing c jets from jets with different quark flavour. The mass ranges in the $m_{\tilde{t}_1}-m_{\tilde{\chi}_1^0}$ plane that are excluded by a search with mono-jet events is shown in figure 15.

6 Current Status

In the previous sections, the experimental status of the SUSY searches after LHC Run 1 were discussed in detail. No statistically significant sign for the existence of supersymmetric particles has been found. Neither did the searches for extended Higgs sectors show any sign of new physics, nor did the precision measurements in the B -meson system. Precision measurements generally show good agreement with the SM prediction, albeit with one potentially interesting development in the cross-section measurement of W^+W^- production (section 6.2). Thus, limits on SUSY have been derived from the direct SUSY searches, either in the form of excluded 2-dimensional hyper-surfaces in a model-parameter space, or in the form of simplified models. But what do these limits mean in terms of the understanding of full physical models of SUSY and *all* their free parameters? How can we apply these limits, and: Taking all available information from all experiments together, can we exclude models of SUSY?

It is the aim of this section to explain the status of SUSY. In section 3.4 we have already detailed how to use the simplified model search limits. Section 6.1 then explains the current status of the global interpretation of SUSY searches and discusses their remaining viability as an explanation of the hierarchy problem, dark matter and the unification of forces. Section 6.2 discusses the interpretation of the interesting (albeit statistically not significant) anomaly of the excess in the W^+W^- cross-section measurement in Run 1 in a SUSY model, and the resulting consequences for future direct searches for SUSY at the LHC. The section closes with a summary of the prospects for the LHC Run 2 in section 6.3.

6.1 Global Fits

If we assume a supersymmetric model with a manageable number of free parameters, we can estimate which regions of parameter space are preferred and which are excluded given our current experimental knowledge. The key observables in such a global parameter fit are the measured Higgs mass and the relic density attributed to the weakly interacting dark-matter agent. If we further assume thermal dark-matter production, the measured relic density requires a sizeable annihilation cross section of the dark-matter states [10, 11]. Given the precision of the Higgs-mass measurement, we also need to include the top mass with appropriate uncertainties as a model parameter. Additional constraints are usually included in our definition of the supersymmetric model: Custodial symmetry will ensure that we are not in conflict with electroweak precision data; a flavour symmetry like minimal flavour violation will keep us away from the rigid flavour constraints in the K and B sectors; leaving out sneutrino dark matter accommodates most of the dark-matter direct-detection constraints.

In the MSSM, the measured Higgs mass gives valuable information on the radiative corrections mentioned in equation (1). The tree-level value as well as the radiative corrections depend on $\tan\beta$. The

leading radiative correction arises from the top-stop sector and involves the same logarithm $\log m_{\tilde{t}}/m_t$ that governs the little hierarchy problem. A relatively heavy Higgs mass requires large stop masses or at least large stop mixing driven by the trilinear coupling A_t introduced in section 2.2. Finally, the plateau value for M_h mentioned in equation (1) will only be reached for heavy additional Higgs states, $M_A > \mathcal{O}(300 \text{ GeV})$.

When we rely on gravity mediation or gauge mediation, we tend to assume that the lightest neutralino is mostly a bino, as discussed in section 2.2. Compared to other compositions of the lightest neutralino the typical bino annihilation cross sections are small, which means they predict too large a relic density. Therefore, scenarios with dominantly bino dark matter have to rely on a mechanism which enhances their annihilation rate. One way would be a very light t -channel state, like for example the $\tilde{\tau}$, mediating the annihilation $\tilde{\chi}_1^0 \tilde{\chi}_1^0 \rightarrow \tau^+ \tau^-$; alternatively, an LSP mass matching the mass of a light Higgs h^0 or heavy Higgs A^0 state combined with enough of a wino component to couple to the Higgs sector will allow for a resonant s -channel annihilation; we can also postulate an additional supersymmetric particle roughly within 10% of the LSP mass to open co-annihilation processes like, e.g., $\tilde{\chi}_1^0 \tilde{f} \rightarrow Z f$ for any Standard Model fermion f [101–104], $\tilde{\chi}_1^0 \tilde{\chi}^+ \rightarrow W^+ Z$ [102, 105, 106], $\tilde{\chi}_1^0 \tilde{\chi}_2^0 \rightarrow W^+ W^-$, or $\tilde{\chi}_1^0 \tilde{\chi}^+ \rightarrow t \bar{b}$. Finally, in the so-called focus point region, or, more generally, the so-called well-tempered neutralino regime of the CMSSM the higgsino mass parameter μ resides close to the point where it crosses zero and changes sign. This way the light LSP receives a sizeable higgsino fraction, which is one way to avoid such co-annihilation channels and generate the observed relic density with the annihilation process $\tilde{\chi}_1^0 \tilde{\chi}_1^0 \rightarrow W^+ W^-$. Similarly, in general models like the pMSSM, the LSP can have a significant wino or higgsino content, enhancing the pair-annihilation rate sufficiently.

A third class of experimental constraints come from indirect searches like the branching ratios for $B_s^0 \rightarrow \mu^+ \mu^-$ and $b \rightarrow s \gamma$, and the anomalous magnetic moment of the muon. The bottom-flavour sector most effectively constrains parameter regions with small heavy Higgs masses and large $\tan \beta > \mathcal{O}(30)$. The measured anomalous magnetic moment of the muon requires light sleptons and light electroweak gauginos. In combination with other measurements this last requirement can be hard to fulfill, which means that the measured anomalous magnetic moment often adds an offset to the quality of the global fits.

Direct LHC searches enter the global fits as limits on the masses (and couplings) of the new states. The LHC limits on the weakly interacting sector are relatively mild. In contrast, the weakly interacting gaugino and slepton sectors are highly sensitive to dark matter observables and, if light, to limits from direct LEP searches. The latter essentially require all new states coupling to the weak gauge sector to have masses above half of the LEP centre-of-mass energy. In the strongly interacting sector the observation of a Higgs boson at a mass far beyond its tree-level bound $M_h < M_Z$ but in agreement with the loop-corrected value of equation (1) points to relatively large squark and gluino masses. This is in general agreement with the non-observation of SUSY in direct searches, so the direct LHC searches will not add much information to a global analysis.

Other constraints, e.g. from possible signals in the search for emissions of neutralino annihilation in the universe, do not enter the global fits. The reason is that possible signals extracted either from γ -ray data [107, 108] or from positron data [109] collected with satellite experiments are subject to significant systematic uncertainties on the astrophysical background, and thus is not necessarily a sign of physics beyond the SM.

Without discussing the technical details, e.g. on the differences in the Bayesian and frequentist approaches to supersymmetric parameter analyses, we will start from the relatively simple CMSSM case and then move towards more general models described in section 2.2. As described above, the main constraints on the supersymmetric parameter space will come from a combination of the Higgs-mass prediction with and the properties of the weakly interacting dark-matter agent. The more constrained the model is, the more clearly we can then identify preferred parameter regions. In particular the dark matter constraint strongly reduces the number of allowed parameter regions, for example in the CMSSM [110–115]: In figure 17(a) we show the profile likelihood in the two mass parameters m_0 and $m_{1/2}$, where the latter largely determines the mass of the LSP. The LHC limits are not included in this figure, so a narrow strip at low but constant $m_{1/2}$ values indicates h^0 -pole annihilation. Such low universal gaugino masses are ruled out by gluino searches at the LHC. The strongly correlated region for $m_{1/2} < 1 \text{ TeV}$ corresponds to stau co-annihilation with a light bino. The absence of the corresponding narrow line-shaped region we see that the focus point region with a light higgsino LSP is essentially ruled out. The bulk region around $m_{1/2} = 1.5 \text{ TeV}$ relies on the heavy Higgs-pole annihilation [110]. It is merged with the so-called well-tempered neutralino scenario, both dominating the allowed CMSSM parameter space.

In this CMSSM parameter study, large values $\tan \beta > 40$ are preferred in order to accommodate the relatively large Higgs-mass value. As expected, the allowed parameter regions by the Higgs mass and the

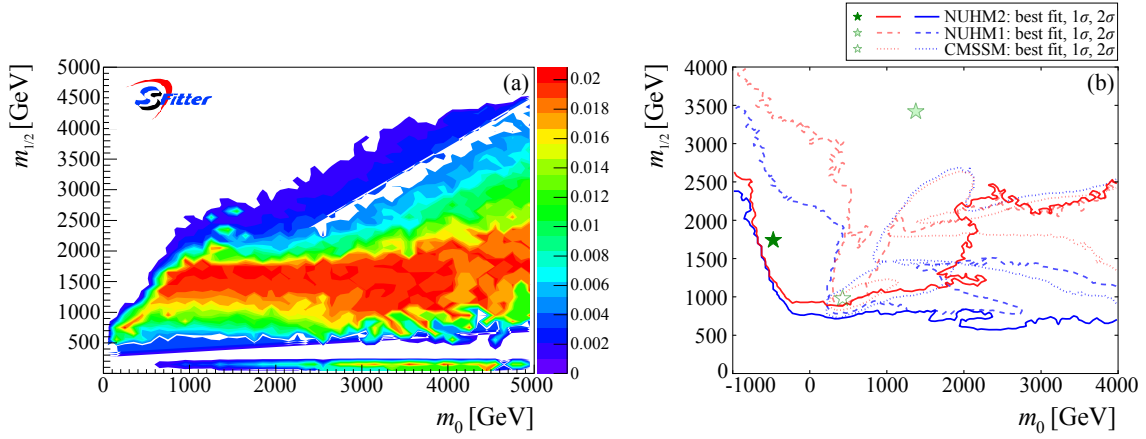


Fig. 17. Fit results in the CMSSM. (a) Frequentist profile likelihood in the m_0 - $m_{1/2}$ plane. (b) Comparison of the CMSSM and the NUHM. (Adapted from Refs. [110, 111].)

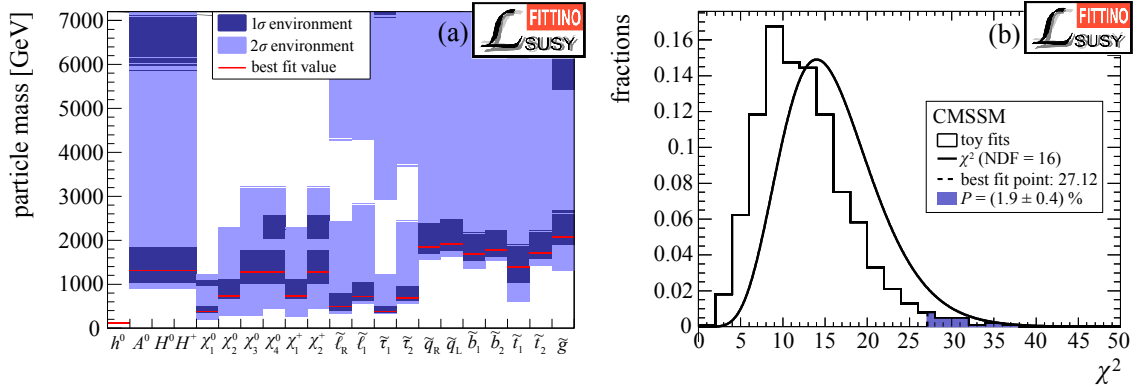


Fig. 18. (a) Mass spectrum for the best-fit point in the CMSSM including error bars. (b) Calculation of the CMSSM p -value below 5% CL. (Adapted from Ref. [115].)

relic density touch the LHC exclusion for low $m_{1/2}$, but the preferred regions are beyond the sensitivity of direct LHC searches (see figure 3). In figure 17(b) a similar result is shown, now based on the NUHM setup introduced in section 2.2. While the best-fit value moves around in the m_0 vs $m_{1/2}$ plane, owing to a relatively flat profile likelihood profile, the qualitative result hardly changes [111].

An interesting question is how well the CMSSM—as one of the most constrained models for the supersymmetric mass spectrum—agrees with all available data in a comprehensive statistical analysis. In figure 18(a) the mass spectrum of the global best-fit parameter point of the MSSM is shown [115]. As expected, gluinos and light-flavour squarks are pushed to high masses. The allowed heavy Higgs states cover a wide range, but also prefer to be heavy. Most of the weakly interacting new states prefer to be light, but are not necessarily accessible in direct production in Run 1. The dark-matter annihilation in this best-fit point proceeds through stau co-annihilation. In figure 18 (b) the statistical analysis of the CMSSM and the corresponding log-likelihoods are shown. The smooth curve shows the naive expectation of the distribution of log-likelihoods, while the histogram shows the actual result from toy experiments. The problem with all CMSSM fits is that slepton and squark masses are linked through the universal scalar mass assumption. Experimentally, the large measured value of the anomalous magnetic moment of the muon prefers light sleptons, while the stronger Higgs-mass constraint prefers heavy squarks. Correspondingly, the overall χ^2 equivalent shows that the quality of the fit is poor and the corresponding p -value is low. In essence, the CMSSM is ruled out at more than 95% CL [115].

This tension in the CMSSM suggests to look at significantly more general, but still predictive parametrisations of SUSY. The biggest challenge in pMSSM parameter studies is to effectively scan the 19-dimensional parameter space [110, 116, 117]. In figure 19 we show the 2-dimensional profile likelihood in the bino–wino mass plane [110]. As for the CMSSM, the dark matter constraint determines the main

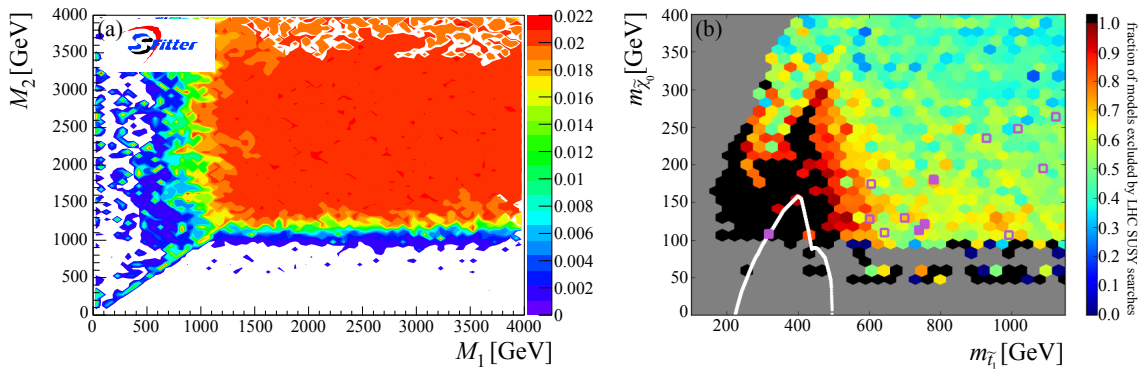


Fig. 19. Fit results in the pMSSM. (a) Frequentist profile likelihood in the bino-wino mass plane before applying LHC results. (b) Fraction of excluded pMSSM models in the LSP- \tilde{t}_1 mass plane. Overlaid is a limit from a simplified-model interpretation. (Adapted from Refs. [110, 116].)

features of the allowed parameter range in the weakly interacting sector. The strongly correlated diagonal strip for $M_1 \sim M_2 \sim 1$ TeV corresponds to stau co-annihilation; the individual points around $M_1 \sim 63$ GeV will at sufficiently large statistics form a line resulting from h^0 -pole annihilation; the bulk region for large M_1 and M_2 receives contributions from heavy Higgs-pole annihilation, or, more generally the well-tempered neutralino scenario including chargino co-annihilation. There exists allowed parameter space for stop co-annihilation, not covered by this specific parameter analysis.

Based on the Higgs-mass constraints a pMSSM analysis can for example map out the preferred parameter space of the extended Higgs sector [118]. One of the most interesting parameter correlations in combination with dark matter then becomes the bino mass vs the lightest stop mass. The former represents the dark matter constraints while the latter probes the Higgs-mass constraints. In figure 19 the fraction of pMSSM parameter points excluded by the LHC searches is shown. Obviously, parameter points with low masses are more often excluded by the searches discussed in section 4. Comparing the contour of constant fraction of rejected points to the contour from a simplified-model interpretation, we observe differences. The reason lies in the assumed decays. On the one hand, actual branching ratios smaller than 100% result in a weaker limit or fewer excluded points than for the simplified model. On the other hand, decay modes not governed by the simplified model can have an enhanced sensitivity and consequently lead to stronger limits or more excluded points. This difference illustrates the problem with simplified model interpretations. Their limits can be applied to all specific SUSY models, but the actual exclusion lines are not the same in complete models. There, the limit might be stronger or weaker, depending on its mass and coupling structure. Note that results based on the fraction of rejected points must be interpreted carefully. First, a scan of a 19-dimensional parameter space is computationally very demanding, so we are not guaranteed that we do not miss allowed points for example at lower masses. An example is the disrupted line of h^0 -pole annihilation in figure 19. Second, the statistical interpretation of the fraction of excluded points includes an ad-hoc Bayesian measure.

The main conclusion of the supersymmetric parameter studies is that including the Higgs measurements of Run 1, the available data on dark matter and indirect constraints, as well as the LHC exclusion bounds the MSSM is not under significant pressure – in strong contrast to the more popular constraint models as the CMSSM. It still offers an explanation for dark matter, for the hierarchy problem, and for approximate gauge coupling unification.

6.2 Experimental Anomalies

From any experiment based on statistical analyses and including significant systematic complexity we should always expect experimental anomalies which lend themselves to new physics interpretations. The crucial test of any anomaly pointing, for example, to physics beyond the Standard Model will be if it becomes more significant when more data are included. A few such anomalies exist at the end of Run 1 at the LHC. They hardly contribute to the global fits, but they maybe interesting to follow up when LHC resumes data taking in 2015.

Already the 7 TeV analyses of W^+W^- production in ATLAS [119] and CMS [120] showed only modest agreement between the data and Standard Model simulations. General problems with this channel,

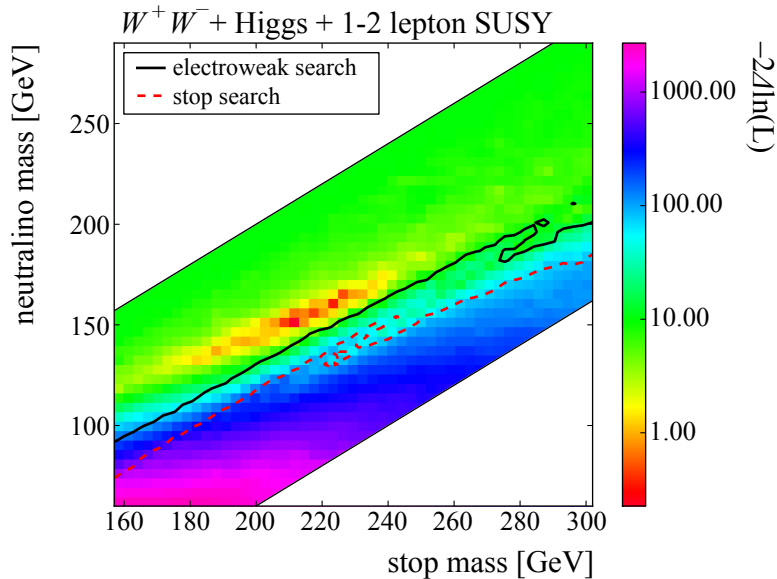


Fig. 20. Two-dimensional likelihood for the relevant mass parameters in the decay chain shown in equation (5). The analysis was performed on ATLAS and CMS W^+W^- measurements. (Adapted from Ref. [122].)

both in the total rate and in some of the distributions, have been known for a long time [121]. The phenomenological analyses of Refs. [122, 123] also includes some CMS 8 TeV results in the same channel [124]. The experimental signature that can be interpreted as Standard Model background plus supersymmetry signal, is dileptons plus missing transverse momentum. The signature includes a jet veto to reject the top-quark pair production background. The assumed signal process is

$$pp \rightarrow \tilde{t}_1 \tilde{t}_1^* \rightarrow (\tilde{\chi}_1^+ b) (\tilde{\chi}_1^- \bar{b}) \rightarrow (\tilde{\chi}_1^0 \ell^+ \nu b) (\tilde{\chi}_1^0 \ell^- \bar{\nu} \bar{b}). \quad (5)$$

This production and decay process is similar to the cascade decay with its dilepton edge discussed in section 2.3. However, rather than through a slepton, the chargino decay proceeds through an off-shell W boson. The final state differs from the W^+W^- background only in the additional existence of two bottom-quark jets. However, as long as the masses of all new particles involved are small and the mass difference does not exceed $m_{\tilde{t}} - m_{\tilde{\chi}^\pm} \sim 7$ GeV, these jets will be too soft to be observable in the general QCD activity of the events. If the mass difference between the stop and the chargino is fixed, the two free parameters in this analysis are the stop mass and the LSP mass. Figure 20 shows the likelihood of a scan of the two-dimensional mass plane. It is dominated by the event count in the signal regions of the three LHC analyses mentioned above. The stop branching ratio to the final state of equation (5) is assumed to be 100%. The strong correlation follows constant mass differences between the stop, the chargino, and the LSP. The best-fit point is

$$m_{\tilde{t}} = 212_{-40}^{+35} \text{ GeV} \quad \text{and} \quad m_{\tilde{\chi}_1^0} = 150_{-20}^{+30} \text{ GeV}.$$

The estimated significance of this single anomaly is around 2.6 standard deviations and can be increased by including tri-lepton signals [122]. The final individual and combined significances will have to be determined in a full experimental analysis.

In a situation like this it is crucial to ensure that the potential signal for new physics is not ruled out by any other LHC searches. For example, searches for direct electroweak gaugino production in the 2-lepton plus missing energy channel contribute to the more constraining of the two exclusion limits shown in figure 20. The second exclusion limit arises from direct stop searches including bottom-quark jets.

As discussed in section 2.3 the invariant mass distribution of two leptons, $m_{\ell\ell}$, is a standard signature for (supersymmetric) cascade decays. Interestingly, there exist indications for such an anomaly in two opposite-sign same-flavor leptons combined with missing transverse momentum both in ATLAS [125] and in CMS [126, 127]. While the ATLAS excess of about 3σ appears directly on the Z^0 resonance at $m_{\ell\ell} = 91.2$ GeV, the CMS excess with a significance of 2.6σ appears as an edge-like structure at $m_{\ell\ell}$ below the Z^0 resonance. As discussed in section 2.3 the main backgrounds can be controlled by opposite-sign

opposite-flavor subtraction. The edge of the corresponding distribution appears around 80 GeV. From this information we can compute the hypersphere of supersymmetric mass values following equation (4).

A sizeable number of events under such an edge points to a strongly interacting hard scattering process. To relate a possible LHC signal to the direct production of light-flavor squarks and gluinos, we have to take into account the limits from generic searches for jets plus missing energy, which only allow heavy light-flavour squarks and gluinos. In comparison, the production rates of third-generation squark pairs are expected to be considerably smaller: First, the light-flavour rates include an additional factor 8 for experimentally indistinguishable squarks, as listed in table 1; second, for light flavours the t -channel gluino exchange contributes up to half of the cross section, while it is strongly suppressed for sbottoms and non-existent for stops. To avoid experimental constraints we could link an observed $m_{\ell\ell}$ edge to the production of relatively light sbottom pairs, $pp \rightarrow \tilde{b}\tilde{b}^*$. The typical supersymmetric parameter range corresponding to such an explanation is similar to the masses required for the WW anomaly discussed above.

Of course, these anomalies could have a number of explanations that are not related to supersymmetry. However, it shows that at the end of Run 1, there are open questions in LHC data which have to be watched in the upcoming runs.

6.3 Prospects for LHC Run 2

As was shown in section 6.1, the CMSSM as the prime example for a constraint SUSY model is at the verge of being completely excluded. However, the exclusion of a single highly constraint model in a global analysis must not be taken as a hint against the realisation of a more general SUSY model. Therefore, also in LHC Run 2, SUSY searches will be of high importance. As motivated in the pMSSM studies in the previous section, special attention will be given to searches for electroweak SUSY partners, sleptons and third-generation squarks. If these remain light (and thus more easily accessible at the LHC), a naturalness problem in the SUSY sector stemming from the difference between the electroweak scale and the mass scale of the SUSY particles can be avoided. Thus gauginos, sleptons and third-generation squarks are prime objectives for the LHC.

As an example of studies for gaugino and top squark searches at higher luminosity, results from ATLAS [128, 129] are shown in figure 21. The existing observed limits derived from the non-observation of SUSY [73, 79] are compared to the expected reach at the LHC with an ultimate integrated luminosity of 300 fb^{-1} and at the HL-LHC with an ultimate integrated luminosity of 3 ab^{-1} . Similar projections exist for CMS [130]. The plots show both the reach for exclusion (dashed) at 95% CL and for a 5σ discovery. It is obvious that already the discovery reach at $\mathcal{L} = 300 \text{ fb}^{-1}$ extends significantly beyond the current exclusion, and thus great discoveries might be expected. However, if the mass scales of SUSY particles in all viable models could be pushed beyond the $\mathcal{O}(\text{TeV})$ region, SUSY would completely lose its attractiveness as an explanation of the hierarchy problem.

The LHC prospects for searches after gluino pair production are also shown in figure 21, both for scenarios with 100% branching ratio of $\tilde{g} \rightarrow q\bar{q}\tilde{\chi}_1^0$ and $\tilde{g} \rightarrow t\bar{t}\tilde{\chi}_1^0$ [130]. In both scenarios the expected discovery reach is extended to 2 TeV and beyond.

On the other hand, the exclusion and discovery potential is still expected to be small for specific mass cases, e.g. for $m_{\tilde{\chi}_2^0} - m_{\tilde{\chi}_1^0} \approx M_Z$ or $m_{\tilde{t}_1} - m_t \approx m_{\tilde{\chi}_1^0}$. In such a case, the momentum of the SM decay particles approaches 0. Therefore, the trigger and selection efficiencies become small and the discovery or exclusion potential can be weakened. The same mechanism applies also to other searches. Thus, it can be expected that also in the unfortunate case of a non-discovery of SUSY in LHC Run 2 and beyond, the fate of SUSY will not be decided by the achievable exclusions directly, but, if at all, by a global analysis looking for SUSY models which fulfill at the same time all constraints from direct searches and all indirect constraints from other sensitive measurements, as outlined in section 6.1.

7 Summary

Although SUSY still is the best-motivated extension of the Standard Model, the LHC Run 1 did not provide us with a clear verdict on its existence. The MSSM still provides explanations for the hierarchy problem and the unification of the forces, as well as for the observation of the SM-like Higgs boson, the cold dark matter in the universe, and for experimental anomalies such as the measurement of the anomalous magnetic moment of the muon $(g-2)_\mu$. All that can be achieved at a mass scale of the lightest SUSY particles of at most a few hundred GeV. The observed Higgs mass, for example, or dark-matter searches could have ruled out the MSSM, but they did not.

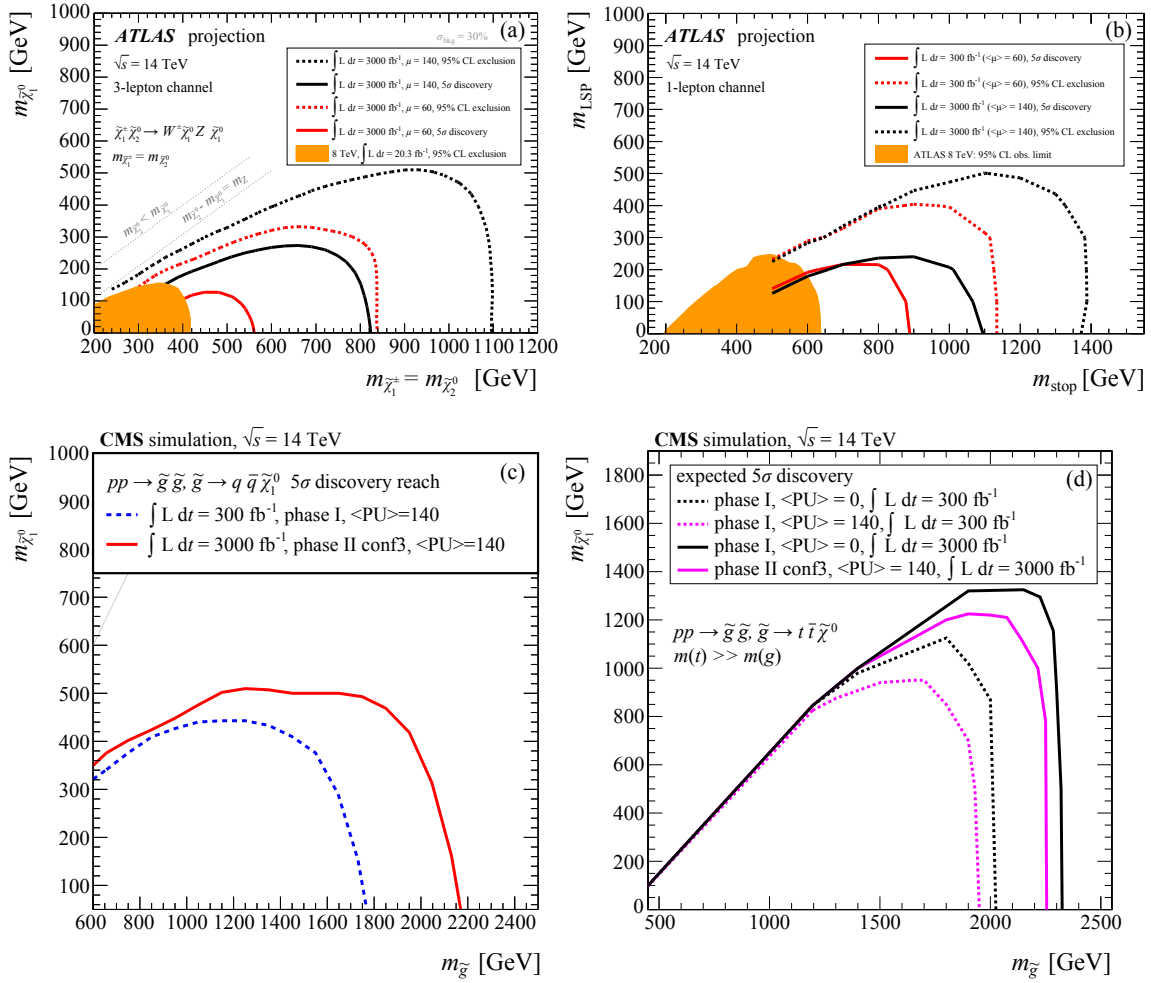


Fig. 21. (a) The expected 95% CL exclusion (dashed lines) and discovery contours (solid lines) for LHC luminosity scenarios with 300 fb⁻¹ (red) and 3000 fb⁻¹ (black) in the $\tilde{\chi}_1^\pm/\tilde{\chi}_2^0-\tilde{\chi}_1^0$ mass plane for a simplified model with 100% branching ratio of $\tilde{\chi}_1^\pm/\tilde{\chi}_2^0 \rightarrow (W/Z)\tilde{\chi}_1^0$ [128]. The measured 8 TeV exclusion contour is displayed as the orange area [73]. (b) Same as (a) but the $\tilde{t}_1-\tilde{\chi}_1^0$ mass plane assuming the decay $\tilde{t}_1 \rightarrow t\tilde{\chi}_1^0$ with a branching ratio of 100% in the 1-lepton decay channel [129]. In addition, the observed excluded region from Ref. [79] is shown. (c) The 5 σ discovery reach for LHC luminosity scenarios with 300 fb⁻¹ (blue dashed line) and 3000 fb⁻¹ (red solid line) in the $\tilde{g}-\tilde{\chi}_1^0$ plane for an assumed 100% branching ratio of $\tilde{g} \rightarrow q\bar{q}\tilde{\chi}_1^0$ [130]. (d) Same as (c) but for a 100% branching ratio of $\tilde{g} \rightarrow q\bar{t}\tilde{\chi}_1^0$, shown for no (black) and realistic (purple) pile-up conditions [130]. (Adapted from Refs. [79, 129, 130].)

No statistically significant hint for new physics has been found in Run 1. The combination of the Higgs-mass measurement and the direct mass limits on SUSY particles on the one hand, and observables like $(g-2)_\mu$ on the other hand have excluded strongly constrained models like the CMSSM at the 95% CL level. This is a great success of combined experimental studies at the LHC, at B factories, at the Tevatron, LEP, from low-energy precision physics, and from cosmology. With the increased energy and luminosity of LHC Run 2, we can expect definite answers on new physics models which include strongly interacting states at the few-TeV scale, including the MSSM.

References

1. T. Schörner-Sadenius, ed., “The Large Hadron Collider — Harvest of Run 1”. Springer, Heidelberg, Germany, 2015.
2. P. W. Higgs, “Broken symmetries, massless particles and gauge fields”, *Phys. Lett.* **12** (1964) 132–133.

3. P. W. Higgs, “Broken Symmetries and the Masses of Gauge Bosons”, *Phys. Rev. Lett.* **13** (1964) 508–509, doi:10.1103/PhysRevLett.13.508.
4. F. Englert and R. Brout, “Broken Symmetry and the Mass of Gauge Vector Mesons”, *Phys. Rev. Lett.* **13** (1964) 321–323, doi:10.1103/PhysRevLett.13.321.
5. CMS Collaboration, “Observation of a new boson at a mass of 125 GeV with the CMS experiment at the LHC”, *Phys. Lett. B* **716** (2012) 30–61, doi:10.1016/j.physletb.2012.08.021, arXiv:1207.7235.
6. ATLAS Collaboration, “Observation of a new particle in the search for the Standard Model Higgs boson with the ATLAS detector at the LHC”, *Phys. Lett. B* **716** (2012) 1–29, doi:10.1016/j.physletb.2012.08.020, arXiv:1207.7214.
7. T. Plehn, “Lectures on LHC Physics”, *Lect. Notes Phys.* **886** (2015) doi:10.1007/978-3-319-05942-6.
8. S. P. Martin, “A Supersymmetry primer”, *Adv. Ser. Direct. High Energy Phys.* **21** (2010) 1–153, doi:10.1142/9789814307505_0001, arXiv:hep-ph/9709356.
9. D. E. Morrissey, T. Plehn, and T. M. Tait, “Physics searches at the LHC”, *Phys. Rept.* **515** (2012) 1–113, doi:10.1016/j.physrep.2012.02.007, arXiv:0912.3259.
10. G. Jungman, M. Kamionkowski, and K. Griest, “Supersymmetric dark matter”, *Phys. Rept.* **267** (1996) 195–373, doi:10.1016/0370-1573(95)00058-5, arXiv:hep-ph/9506380.
11. G. Bertone, D. Hooper, and J. Silk, “Particle dark matter: Evidence, candidates and constraints”, *Phys. Rept.* **405** (2005) 279–390, doi:10.1016/j.physrep.2004.08.031, arXiv:hep-ph/0404175.
12. W. Bernreuther, “CP violation and baryogenesis”, *Lect. Notes Phys.* **591** (2002) 237–293, arXiv:hep-ph/0205279.
13. U. Amaldi, W. de Boer, and H. Furstenau, “Comparison of grand unified theories with electroweak and strong coupling constants measured at LEP”, *Phys. Lett. B* **260** (1991) 447–455, doi:10.1016/0370-2693(91)91641-8.
14. E. Gildener, “Gauge Symmetry Hierarchies”, *Phys. Rev. D* **14** (1976) 1667, doi:10.1103/PhysRevD.14.1667.
15. S. Weinberg, “Implications of Dynamical Symmetry Breaking”, *Phys. Rev. D* **13** (1976) 974–996, doi:10.1103/PhysRevD.13.974.
16. B. W. Lee, C. Quigg, and H. Thacker, “The Strength of Weak Interactions at Very High-Energies and the Higgs Boson Mass”, *Phys. Rev. Lett.* **38** (1977) 883–885, doi:10.1103/PhysRevLett.38.883.
17. Y. Golfand and E. Likhtman, “Extension of the Algebra of Poincare Group Generators and Violation of p Invariance”, *JETP Lett.* **13** (1971) 323–326.
18. D. Volkov and V. Akulov, “Possible universal neutrino interaction”, *JETP Lett.* **16** (1972) 438–440.
19. J. Wess and B. Zumino, “Supergauge Transformations in Four-Dimensions”, *Nucl. Phys. B* **70** (1974) 39–50, doi:10.1016/0550-3213(74)90355-1.
20. A. Salam and J. Strathdee, “Supergauge Transformations”, *Nucl. Phys. B* **76** (1974) 477–482, doi:10.1016/0550-3213(74)90537-9.
21. R. Haag, J. T. Lopuszanski, and M. Sohnius, “All Possible Generators of Supersymmetries of the s Matrix”, *Nucl. Phys. B* **88** (1975) 257, doi:10.1016/0550-3213(75)90279-5.
22. J. Wess and J. Bagger, “Supersymmetry and Supergravity”. Princeton University Press, Princeton, USA, 1992.
23. J. Terning, “Modern Supersymmetry: Dynamics and Duality”. Oxford University Press, Oxford, United Kingdom, 2006.
24. M. Drees, R. Godbole, and P. Roy, “Theory and phenomenology of sparticles: An account of four-dimensional N=1 supersymmetry in high energy physics”. World Scientific, Hackensack, USA, 2004.
25. H. Baer and X. Tata, “Weak Scale Supersymmetry: From Superfields to Scattering Events”. Cambridge University Press, Cambridge, United Kingdom, 2006.
26. S. Dawson and H. Georgi, “GENERALIZED GAUGE HIERARCHIES”, *Phys. Rev. Lett.* **43** (1979) 821, doi:10.1103/PhysRevLett.43.821.
27. M. Einhorn and D. Jones, “The Weak Mixing Angle and Unification Mass in Supersymmetric SU(5)”, *Nucl. Phys. B* **196** (1982) 475, doi:10.1016/0550-3213(82)90502-8.
28. S. Dimopoulos and H. Georgi, “Softly Broken Supersymmetry and SU(5)”, *Nucl. Phys. B* **193** (1981) 150, doi:10.1016/0550-3213(81)90522-8.

29. M. Dine and W. Fischler, “A Phenomenological Model of Particle Physics Based on Supersymmetry”, *Phys. Lett. B* **110** (1982) 227, doi:10.1016/0370-2693(82)91241-2.
30. G. R. Farrar and P. Fayet, “Phenomenology of the Production, Decay, and Detection of New Hadronic States Associated with Supersymmetry”, *Phys. Lett. B* **76** (1978) 575–579, doi:10.1016/0370-2693(78)90858-4.
31. H. K. Dreiner, “An Introduction to explicit R-parity violation”, *Adv. Ser. Direct. High Energy Phys.* **21** (2010) 565–583, doi:10.1142/9789814307505_0017, arXiv:hep-ph/9707435.
32. J. F. Gunion, H. E. Haber, G. L. Kane, and S. Dawson, “The Higgs Hunter’s Guide”, *Front. Phys.* **80** (2000) 1–448.
33. A. Djouadi, “The Anatomy of electro-weak symmetry breaking. II. The Higgs bosons in the minimal supersymmetric model”, *Phys. Rept.* **459** (2008) 1–241, doi:10.1016/j.physrep.2007.10.005, arXiv:hep-ph/0503173.
34. P. H. Chankowski, S. Pokorski, and J. Rosiek, “Complete on-shell renormalization scheme for the minimal supersymmetric Higgs sector”, *Nucl. Phys. B* **423** (1994) 437–496, doi:10.1016/0550-3213(94)90141-4, arXiv:hep-ph/9303309.
35. H. E. Haber and R. Hempfling, “The Renormalization group improved Higgs sector of the minimal supersymmetric model”, *Phys. Rev. D* **48** (1993) 4280–4309, doi:10.1103/PhysRevD.48.4280, arXiv:hep-ph/9307201.
36. R. Hempfling and A. H. Hoang, “Two loop radiative corrections to the upper limit of the lightest Higgs boson mass in the minimal supersymmetric model”, *Phys. Lett. B* **331** (1994) 99–106, doi:10.1016/0370-2693(94)90948-2, arXiv:hep-ph/9401219.
37. M. Carena et al., “Reconciling the two loop diagrammatic and effective field theory computations of the mass of the lightest CP - even Higgs boson in the MSSM”, *Nucl. Phys. B* **580** (2000) 29–57, doi:10.1016/S0550-3213(00)00212-1, arXiv:hep-ph/0001002.
38. L. Girardello and M. T. Grisaru, “Soft Breaking of Supersymmetry”, *Nucl. Phys. B* **194** (1982) 65, doi:10.1016/0550-3213(82)90512-0.
39. H. Goldberg, “Constraint on the Photino Mass from Cosmology”, *Phys. Rev. Lett.* **50** (1983) 1419, doi:10.1103/PhysRevLett.50.1419.
40. J. R. Ellis et al., “Supersymmetric Relics from the Big Bang”, *Nucl. Phys. B* **238** (1984) 453–476, doi:10.1016/0550-3213(84)90461-9.
41. J. Jaeckel, V. V. Khoze, T. Plehn, and P. Richardson, “Travels on the squark-gluino mass plane”, *Phys. Rev. D* **85** (2012) 015015, doi:10.1103/PhysRevD.85.015015, arXiv:1109.2072.
42. N. Arkani-Hamed and S. Dimopoulos, “Supersymmetric unification without low energy supersymmetry and signatures for fine-tuning at the LHC”, *JHEP* **06** (2005) 073, doi:10.1088/1126-6708/2005/06/073, arXiv:hep-th/0405159.
43. G. Giudice and A. Romanino, “Split supersymmetry”, *Nucl. Phys. B* **699** (2004) 65–89, doi:10.1016/j.nuclphysb.2004.11.048, arXiv:hep-ph/0406088.
44. L. E. Ibanez and G. G. Ross, “Low-Energy Predictions in Supersymmetric Grand Unified Theories”, *Phys. Lett. B* **105** (1981) 439, doi:10.1016/0370-2693(81)91200-4.
45. A. H. Chamseddine, R. L. Arnowitt, and P. Nath, “Locally Supersymmetric Grand Unification”, *Phys. Rev. Lett.* **49** (1982) 970, doi:10.1103/PhysRevLett.49.970.
46. R. Barbieri, S. Ferrara, and C. A. Savoy, “Gauge Models with Spontaneously Broken Local Supersymmetry”, *Phys. Lett. B* **119** (1982) 343, doi:10.1016/0370-2693(82)90685-2.
47. M. Dine, W. Fischler, and M. Srednicki, “Supersymmetric Technicolor”, *Nucl. Phys. B* **189** (1981) 575–593, doi:10.1016/0550-3213(81)90582-4.
48. S. Dimopoulos and S. Raby, “Supercolor”, *Nucl. Phys. B* **192** (1981) 353, doi:10.1016/0550-3213(81)90430-2.
49. M. Kramer et al., “Supersymmetry production cross sections in pp collisions at $\sqrt{s} = 7$ TeV”, arXiv:1206.2892.
50. CMS Collaboration, “Search for new physics in the multijet and missing transverse momentum final state in proton-proton collisions at $\sqrt{s} = 8$ TeV”, *JHEP* **06** (2014) 055, doi:10.1007/JHEP06(2014)055, arXiv:1402.4770.
51. ATLAS Collaboration, “Search for squarks and gluinos with the ATLAS detector in final states with jets and missing transverse momentum using $\sqrt{s} = 8$ TeV proton-proton collision data”, *JHEP* **09** (2014) 176, doi:10.1007/JHEP09(2014)176, arXiv:1405.7875.
52. ATLAS Collaboration, “Search for supersymmetry at $\sqrt{s} = 8$ TeV in final states with jets and two same-sign leptons or three leptons with the ATLAS detector”, *JHEP* **06** (2014) 035, doi:10.1007/JHEP06(2014)035, arXiv:1404.2500.

53. L. Randall and D. Tucker-Smith, “Dijet Searches for Supersymmetry at the LHC”, *Phys. Rev. Lett.* **101** (2008) 221803, doi:10.1103/PhysRevLett.101.221803, arXiv:0806.1049.
54. CMS Collaboration, “Search for supersymmetry in hadronic final states with missing transverse energy using the variables AlphaT and b-quark multiplicity in pp collisions at 8 TeV”, *Eur. Phys. J. C* **73** (2013) 2568, doi:10.1140/epjc/s10052-013-2568-6, arXiv:1303.2985.
55. CMS Collaboration, “Inclusive search for supersymmetry using the razor variables in pp collisions at $\sqrt{s} = 7$ TeV”, *Phys. Rev. Lett.* **111** (2013), no. 8, 081802, doi:10.1103/PhysRevLett.111.081802, arXiv:1212.6961.
56. C. Lester and D. Summers, “Measuring masses of semiinvisibly decaying particles pair produced at hadron colliders”, *Phys. Lett. B* **463** (1999) 99–103, doi:10.1016/S0370-2693(99)00945-4, arXiv:hep-ph/9906349.
57. A. Barr, C. Lester, and P. Stephens, “m(T2): The Truth behind the glamour”, *J. Phys. G* **29** (2003) 2343–2363, doi:10.1088/0954-3899/29/10/304, arXiv:hep-ph/0304226.
58. CMS Collaboration, “Search for supersymmetry in hadronic final states using MT2 in pp collisions at $\sqrt{s} = 7$ TeV”, *JHEP* **10** (2012) 018, doi:10.1007/JHEP10(2012)018, arXiv:1207.1798.
59. CMS Collaboration, “Searches for supersymmetry using the M_{T2} variable in hadronic events produced in pp collisions at 8 TeV”, arXiv:1502.04358.
60. ATLAS Collaboration, “Further search for supersymmetry at $\sqrt{s} = 7$ TeV in final states with jets, missing transverse momentum and isolated leptons with the ATLAS detector”, *Phys. Rev. D* **86** (2012) 092002, doi:10.1103/PhysRevD.86.092002, arXiv:1208.4688.
61. CMS Collaboration, “Search for supersymmetry in pp collisions at $\sqrt{s} = 7$ TeV in events with a single lepton, jets, and missing transverse momentum”, *Eur. Phys. J. C* **73** (2013) 2404, doi:10.1140/epjc/s10052-013-2404-z, arXiv:1212.6428.
62. CMS Collaboration, “Search for new physics in events with same-sign dileptons and jets in pp collisions at $\sqrt{s} = 8$ TeV”, *JHEP* **01** (2014) 163, doi:10.1007/JHEP01(2014)163, arXiv:1311.6736.
63. CMS Collaboration, “Search for physics beyond the standard model in events with τ leptons, jets, and large transverse momentum imbalance in pp collisions at $\sqrt{s} = 7$ TeV”, *Eur. Phys. J. C* **73** (2013) 2493, doi:10.1140/epjc/s10052-013-2493-8, arXiv:1301.3792.
64. ATLAS Collaboration, “Search for Supersymmetry in Events with Large Missing Transverse Momentum, Jets, and at Least One Tau Lepton in 7 TeV Proton-Proton Collision Data with the ATLAS Detector”, *Eur. Phys. J. C* **72** (2012) 2215, doi:10.1140/epjc/s10052-012-2215-7, arXiv:1210.1314.
65. ATLAS Collaboration, “Search for supersymmetry in events with large missing transverse momentum, jets, and at least one tau lepton in 20 fb⁻¹ of $\sqrt{s} = 8$ TeV proton-proton collision data with the ATLAS detector”, *JHEP* **09** (2014) 103, doi:10.1007/JHEP09(2014)103, arXiv:1407.0603.
66. CMS Collaboration, “Search for anomalous production of events with three or more leptons in pp collisions at $\sqrt{s} = 8$ TeV”, *Phys. Rev. D* **90** (2014) 032006, doi:10.1103/PhysRevD.90.032006, arXiv:1404.5801.
67. S. Dimopoulos, S. D. Thomas, and J. D. Wells, “Sparticle spectroscopy and electroweak symmetry breaking with gauge mediated supersymmetry breaking”, *Nucl. Phys. B* **488** (1997) 39–91, doi:10.1016/S0550-3213(97)00030-8, arXiv:hep-ph/9609434.
68. P. Meade, N. Seiberg, and D. Shih, “General Gauge Mediation”, *Prog. Theor. Phys. Suppl.* **177** (2009) 143–158, doi:10.1143/PTPS.177.143, arXiv:0801.3278.
69. ATLAS Collaboration, “Search for diphoton events with large missing transverse momentum in 7 TeV proton-proton collision data with the ATLAS detector”, *Phys. Lett. B* **718** (2012) 411–430, doi:10.1016/j.physletb.2012.10.069, arXiv:1209.0753.
70. CMS Collaboration, “Search for new physics in events with photons, jets, and missing transverse energy in pp collisions at $\sqrt{s} = 7$ TeV”, *JHEP* **03** (2013) 111, doi:10.1007/JHEP03(2013)111, arXiv:1211.4784.
71. CMS Collaboration, “Interpretation of Searches for Supersymmetry with simplified Models”, *Phys. Rev. D* **88** (2013), no. 5, 052017, doi:10.1103/PhysRevD.88.052017, arXiv:1301.2175.
72. ATLAS Collaboration, “Search for direct production of charginos and neutralinos in events with three leptons and missing transverse momentum in $\sqrt{s} = 8$ TeV pp collisions with the ATLAS detector”, *JHEP* **04** (2014) 169, doi:10.1007/JHEP04(2014)169, arXiv:1402.7029.
73. ATLAS Collaboration, “Search for direct production of charginos, neutralinos and sleptons in final states with two leptons and missing transverse momentum in pp collisions at $\sqrt{s} = 8$ TeV with the ATLAS detector”, *JHEP* **05** (2014) 071, doi:10.1007/JHEP05(2014)071, arXiv:1403.5294.

74. ATLAS Collaboration, “Search for supersymmetry in events with four or more leptons in $\sqrt{s} = 8$ TeV pp collisions with the ATLAS detector”, *Phys. Rev. D* **90** (2014) 052001, doi:10.1103/PhysRevD.90.052005, 10.1103/PhysRevD.90.052001, arXiv:1405.5086.
75. ATLAS Collaboration, “Search for the direct production of charginos, neutralinos and staus in final states with at least two hadronically decaying taus and missing transverse momentum in pp collisions at $\sqrt{s} = 8$ TeV with the ATLAS detector”, *JHEP* **10** (2014) 96, doi:10.1007/JHEP10(2014)096, arXiv:1407.0350.
76. CMS Collaboration, “Searches for electroweak production of charginos, neutralinos, and sleptons decaying to leptons and W, Z, and Higgs bosons in pp collisions at 8 TeV”, *Eur. Phys. J. C* **74** (2014), no. 9, 3036, doi:10.1140/epjc/s10052-014-3036-7, arXiv:1405.7570.
77. CMS Collaboration, “Searches for electroweak neutralino and chargino production in channels with Higgs, Z, and W bosons in pp collisions at 8 TeV”, *Phys.Rev.* **D90** (2014), no. 9, 092007, doi:10.1103/PhysRevD.90.092007, arXiv:1409.3168.
78. CMS Collaboration, “Search for top squark and higgsino production using diphoton Higgs boson decays”, *Phys. Rev. Lett.* **112** (2014) 161802, doi:10.1103/PhysRevLett.112.161802, arXiv:1312.3310.
79. ATLAS Collaboration, “Search for top squark pair production in final states with one isolated lepton, jets, and missing transverse momentum in $\sqrt{s} = 8$ TeV pp collisions with the ATLAS detector”, *JHEP* **1411** (2014) 118, doi:10.1007/JHEP11(2014)118, arXiv:1407.0583.
80. CMS Collaboration, “Search for top-squark pair production in the single-lepton final state in pp collisions at $\sqrt{s} = 8$ TeV”, *Eur. Phys. J. C* **73** (2013) 2677, doi:10.1140/epjc/s10052-013-2677-2, arXiv:1308.1586.
81. ATLAS Collaboration, “Search for direct third-generation squark pair production in final states with missing transverse momentum and two b-jets in $\sqrt{s} = 8$ TeV pp collisions with the ATLAS detector”, *JHEP* **10** (2013) 189, doi:10.1007/JHEP10(2013)189, arXiv:1308.2631.
82. ATLAS Collaboration, “Search for direct top-squark pair production in final states with two leptons in pp collisions at $\sqrt{s} = 8$ TeV with the ATLAS detector”, *JHEP* **06** (2014) 124, doi:10.1007/JHEP06(2014)124, arXiv:1403.4853.
83. ATLAS Collaboration, “Search for direct top squark pair production in events with a Z boson, b-jets and missing transverse momentum in sqrt(s)=8 TeV pp collisions with the ATLAS detector”, *Eur. Phys. J. C* **74** (2014) 2883, doi:10.1140/epjc/s10052-014-2883-6, arXiv:1403.5222.
84. ATLAS Collaboration, “Search for direct pair production of the top squark in all-hadronic final states in proton-proton collisions at $\sqrt{s} = 8$ TeV with the ATLAS detector”, *JHEP* **09** (2014) 015, doi:10.1007/JHEP09(2014)015, arXiv:1406.1122.
85. ATLAS Collaboration, “Measurement of the $t\bar{t}$ production cross-section using $e\mu$ events with b-tagged jets in pp collisions at $\sqrt{s} = 7$ and 8 TeV with the ATLAS detector”, *Eur. Phys. J. C* **74** (2014), no. 10, 3109, doi:10.1140/epjc/s10052-014-3109-7, arXiv:1406.5375.
86. ATLAS Collaboration, “Search for strong production of supersymmetric particles in final states with missing transverse momentum and at least three b-jets at $\sqrt{s} = 8$ TeV proton-proton collisions with the ATLAS detector”, *JHEP* **10** (2014) 24, doi:10.1007/JHEP10(2014)024, arXiv:1407.0600.
87. ATLAS Collaboration, “Search for pair-produced third-generation squarks decaying via charm quarks or in compressed supersymmetric scenarios in pp collisions at $\sqrt{s} = 8$ TeV with the ATLAS detector”, *Phys. Rev. D* **90** (2014) 052008, doi:10.1103/PhysRevD.90.052008, arXiv:1407.0608.
88. J. M. Butterworth, A. R. Davison, M. Rubin, and G. P. Salam, “Jet substructure as a new Higgs search channel at the LHC”, *Phys. Rev. Lett.* **100** (2008) 242001, doi:10.1103/PhysRevLett.100.242001, arXiv:0802.2470.
89. ATLAS Collaboration, “Performance of jet substructure techniques for large-R jets in proton-proton collisions at $\sqrt{s} = 7$ TeV using the ATLAS detector”, *JHEP* **09** (2013) 076, doi:10.1007/JHEP09(2013)076, arXiv:1306.4945.
90. D. Krohn, J. Thaler, and L.-T. Wang, “Jet Trimming”, *JHEP* **02** (2010) 084, doi:10.1007/JHEP02(2010)084, arXiv:0912.1342.
91. ATLAS Collaboration, “Search for a supersymmetric partner to the top quark in final states with jets and missing transverse momentum at $\sqrt{s} = 7$ TeV with the ATLAS detector”, *Phys. Rev. Lett.* **109** (2012) 211802, doi:10.1103/PhysRevLett.109.211802, arXiv:1208.1447.
92. ATLAS Collaboration, “Search for direct top squark pair production in final states with one isolated lepton, jets, and missing transverse momentum in $\sqrt{s} = 7$ TeV pp collisions using $4.7 fb^{-1}$ ”,

- of ATLAS data”, *Phys. Rev. Lett.* **109** (2012) 211803, doi:10.1103/PhysRevLett.109.211803, arXiv:1208.2590.
93. ATLAS Collaboration, “Search for a heavy top-quark partner in final states with two leptons with the ATLAS detector at the LHC”, *JHEP* **11** (2012) 094, doi:10.1007/JHEP11(2012)094, arXiv:1209.4186.
94. ATLAS Collaboration, “Search for long-lived stopped R-hadrons decaying out-of-time with pp collisions using the ATLAS detector”, *Phys. Rev. D* **88** (2013), no. 11, 112003, doi:10.1103/PhysRevD.88.112003, arXiv:1310.6584.
95. CMS Collaboration, “Search for stopped long-lived particles produced in pp collisions at $\sqrt{s} = 7$ TeV”, *JHEP* **08** (2012) 026, doi:10.1007/JHEP08(2012)026, arXiv:1207.0106.
96. ATLAS Collaboration, “Search for charginos nearly mass degenerate with the lightest neutralino based on a disappearing-track signature in pp collisions at $\sqrt{s}=8$ TeV with the ATLAS detector”, *Phys. Rev. D* **88** (2013), no. 11, 112006, doi:10.1103/PhysRevD.88.112006, arXiv:1310.3675.
97. S. Weinberg, “Supersymmetry at Ordinary Energies. 1. Masses and Conservation Laws”, *Phys. Rev. D* **26** (1982) 287, doi:10.1103/PhysRevD.26.287.
98. N. Sakai and T. Yanagida, “Proton Decay in a Class of Supersymmetric Grand Unified Models”, *Nucl. Phys. B* **197** (1982) 533, doi:10.1016/0550-3213(82)90457-6.
99. SNO Collaboration, “Constraints on nucleon decay via ‘invisible’ modes from the Sudbury Neutrino Observatory”, *Phys. Rev. Lett.* **92** (2004) 102004, doi:10.1103/PhysRevLett.92.102004, arXiv:hep-ex/0310030.
100. S. P. Martin, “Compressed supersymmetry and natural neutralino dark matter from top squark-mediated annihilation to top quarks”, *Phys. Rev. D* **75** (2007) 115005, doi:10.1103/PhysRevD.75.115005, arXiv:hep-ph/0703097.
101. K. Griest and D. Seckel, “Three exceptions in the calculation of relic abundances”, *Phys. Rev. D* **43** (1991) 3191–3203, doi:10.1103/PhysRevD.43.3191.
102. S. Mizuta and M. Yamaguchi, “Coannihilation effects and relic abundance of Higgsino dominant LSP(s)”, *Phys. Lett. B* **298** (1993) 120–126, doi:10.1016/0370-2693(93)91717-2, arXiv:hep-ph/9208251.
103. J. R. Ellis, T. Falk, and K. A. Olive, “Neutralino - Stau coannihilation and the cosmological upper limit on the mass of the lightest supersymmetric particle”, *Phys. Lett. B* **444** (1998) 367–372, doi:10.1016/S0370-2693(98)01392-6, arXiv:hep-ph/9810360.
104. J. R. Ellis, K. A. Olive, and Y. Santoso, “Calculations of neutralino stop coannihilation in the CMSSM”, *Astropart. Phys.* **18** (2003) 395–432, doi:10.1016/S0927-6505(02)00151-2, arXiv:hep-ph/0112113.
105. P. Binetruy, G. Girardi, and P. Salati, “Constraints on a System of Two Neutral Fermions From Cosmology”, *Nucl. Phys. B* **237** (1984) 285, doi:10.1016/0550-3213(84)90161-5.
106. J. Edsjo and P. Gondolo, “Neutralino relic density including coannihilations”, *Phys. Rev. D* **56** (1997) 1879–1894, doi:10.1103/PhysRevD.56.1879, arXiv:hep-ph/9704361.
107. LAT Collaboration, “Fermi LAT Search for Dark Matter in Gamma-ray Lines and the Inclusive Photon Spectrum”, *Phys. Rev. D* **86** (2012) 022002, doi:10.1103/PhysRevD.86.022002, arXiv:1205.2739.
108. C. Weniger, “A Tentative Gamma-Ray Line from Dark Matter Annihilation at the Fermi Large Area Telescope”, *JCAP* **1208** (2012) 007, doi:10.1088/1475-7516/2012/08/007, arXiv:1204.2797.
109. PAMELA Collaboration, “Cosmic-Ray Positron Energy Spectrum Measured by PAMELA”, *Phys. Rev. Lett.* **111** (2013), no. 8, 081102, doi:10.1103/PhysRevLett.111.081102, arXiv:1308.0133.
110. S. Henrot-Versillé et al., “Constraining Supersymmetry using the relic density and the Higgs boson”, *Phys. Rev. D* **89** (2014) 055017, arXiv:1309.6958.
111. O. Buchmueller et al., “The NUHM2 after LHC Run 1”, *Eur.Phys.J.* **C74** (2014), no. 12, 3212, doi:10.1140/epjc/s10052-014-3212-9, arXiv:1408.4060.
112. C. Strege et al., “Global Fits of the cMSSM and NUHM including the LHC Higgs discovery and new XENON100 constraints”, *JCAP* **1304** (2013) 013, doi:10.1088/1475-7516/2013/04/013, arXiv:1212.2636.
113. T. Cohen and J. G. Wacker, “Here be Dragons: The Unexplored Continents of the CMSSM”, *JHEP* **09** (2013) 061, doi:10.1007/JHEP09(2013)061, arXiv:1305.2914.
114. L. Roszkowski, E. M. Sessolo, and A. J. Williams, “What next for the CMSSM and the NUHM: Improved prospects for superpartner and dark matter detection”, *JHEP* **08** (2014) 067, doi:10.1007/JHEP08(2014)067, arXiv:1405.4289.
115. P. Bechtle et al., “How alive is constrained SUSY really?”, arXiv:1410.6035.

116. M. W. Cahill-Rowley, J. L. Hewett, A. Ismail, and T. G. Rizzo, “More energy, more searches, but the phenomenological MSSM lives on”, *Phys. Rev. D* **88** (2013), no. 3, 035002, doi:10.1103/PhysRevD.88.035002, arXiv:1211.1981.
117. C. Boehm, P. S. B. Dev, A. Mazumdar, and E. Pukartas, “Naturalness of Light Neutralino Dark Matter in pMSSM after LHC, XENON100 and Planck Data”, *JHEP* **06** (2013) 113, doi:10.1007/JHEP06(2013)113, arXiv:1303.5386.
118. B. Dumont, J. F. Gunion, and S. Kraml, “The phenomenological MSSM in view of the 125 GeV Higgs data”, *Phys. Rev. D* **89** (2014) 055018, doi:10.1103/PhysRevD.89.055018, arXiv:1312.7027.
119. ATLAS Collaboration, “Measurement of W^+W^- production in pp collisions at $\sqrt{s}=7\text{TeV}$ with the ATLAS detector and limits on anomalous WWZ and WW couplings”, *Phys. Rev. D* **87** (2013), no. 11, 112001, doi:10.1103/PhysRevD.87.112001, 10.1103/PhysRevD.88.079906, arXiv:1210.2979.
120. CMS Collaboration, “Measurement of the W^+W^- Cross section in pp Collisions at $\sqrt{s} = 7$ TeV and Limits on Anomalous $WW\gamma$ and WWZ couplings”, *Eur. Phys. J. C* **73** (2013) 2610, doi:10.1140/epjc/s10052-013-2610-8, arXiv:1306.1126.
121. D. Curtin, P. Jaiswal, and P. Meade, “Charginos Hiding In Plain Sight”, *Phys. Rev. D* **87** (2013), no. 3, 031701, doi:10.1103/PhysRevD.87.031701, arXiv:1206.6888.
122. J. S. Kim, K. Rolbiecki, K. Sakurai, and J. Tattersall, “‘Stop’ that ambulance! New physics at the LHC?”, *JHEP* **1412** (2014) 010, doi:10.1007/JHEP12(2014)010, arXiv:1406.0858.
123. D. Curtin, P. Meade, and P.-J. Tien, “Natural SUSY in Plain Sight”, *Phys.Rev.* **D90** (2014), no. 11, 115012, doi:10.1103/PhysRevD.90.115012, arXiv:1406.0848.
124. CMS Collaboration, “Measurement of W^+W^- and ZZ production cross sections in pp collisions at $\sqrt{s} = 8$ TeV”, *Phys. Lett. B* **721** (2013) 190–211, doi:10.1016/j.physletb.2013.03.027, arXiv:1301.4698.
125. ATLAS Collaboration, “Search for supersymmetry in events containing a same-flavour opposite-sign dilepton pair, jets, and large missing transverse momentum in $\sqrt{s} = 8$ TeV pp collisions with the ATLAS detector”, arXiv:1503.03290.
126. CMS Collaboration, “Search for physics beyond the standard model in events with two leptons, jets, and missing transverse momentum in pp collisions at $\sqrt{s} = 8$ TeV”, arXiv:1502.06031.
127. B. Allanach, A. R. Raklev, and A. Kvellestad, “Interpreting a CMS $lljjp_T^{\text{miss}}$ Excess With the Golden Cascade of the MSSM”, arXiv:1409.3532.
128. ATLAS Collaboration, “Search for Supersymmetry at the high luminosity LHC with the ATLAS experiment”. ATL-PHYS-PUB-2014-010.
129. ATLAS Collaboration, “Prospects for benchmark Supersymmetry searches at the high luminosity LHC with the ATLAS Detector”. ATL-PHYS-PUB-2013-011.
130. CMS Collaboration, “Projected Performance of an Upgraded CMS Detector at the LHC and HL-LHC: Contribution to the Snowmass Process”, arXiv:1307.7135.